Attachment 3.: Statement of Research Activity

1 First name and surname

Krzysztof Wohlfeld

2 Diplomas, degrees or artistic degrees with the name, place and year of obtaining them and the title of the doctoral dissertation.

(a) Master of science in theoretical physics: Jagellonian University, Cracow, June 2005 (with distinction). Master thesis entitled "Double exchange model for degenerate t_{2g} orbitals" (supervisor: professor Andrzej M. Oleś).

(b) PhD in physical sciences: Jagellonian University, Cracow, June 2009 (with distinction). PhD thesis entitled "Beyond the standard t–J model" (supervisor: professor Andrzej M. Oleś).

3 Information on previous employment in scientific or artistic units:

(a) Postdoc in the group of professor Jeroen van den Brinka in the Leibniz-Institut für Festkörper- und Werkstoffforschung Dresden (IFW); October 2009 - October 2012; from May 2010 till May 2012 as an Alexander von Humboldt fellow.

(b) Postdoc in the group of professor Thomas P. Devereaux in the Stanford Institute for Materials and Energy Sciences (joint institute of Stanford University and SLAC National Accelerator Laboratory); November 2012 - February 2015.

(c) Assistant Professor in the Chair of Condensed Matter Physics of the Insitute for Theoretical Physics of the Faculty of Physics of the University of Warsaw (since February 2015).

4 Indication of achievement resulting from art. 16 sec. 2 of the Act of 14 March 2003 on academic degrees and academic title, and degrees and title in the field of art (Journal of Laws No. 65, item 595 with changes):

(a) Title of the scientific achievement

series of articles: "Propagation of an Orbiton in an Antiferromagnet"

(b) (authors, title, publication date, name of publisher)

[H1] **K. Wohlfeld**, M. Daghofer, S. Nishimoto, G. Khaliullin, J. van den Brink, "Intrinsic Coupling of Orbital Excitations to Spin Fluctuations in Mott Insulators", Physical Review Letters **107**, 147201 (2011).

[H2] J. Schlappa, **K. Wohlfeld**, K. J. Zhou, M. Mourigal, M. W. Haverkort, V. N. Strocov, L. Hozoi, C. Monney, S. Nishimoto, S. Singh, A. Revcolevschi, J.-S. Caux, L. Patthey, H. M. Ronnow, J. van den Brink, T. Schmitt, "Spin-Orbital Separation in the quasi 1D Mott-insulator Sr_2CuO_3", Nature **485**, 82 (2012).

[H3] **K. Wohlfeld**, M. Daghofer, G. Khaliullin, J. van den Brink, "Dispersion of orbital excitations in 2D quantum antiferromagnets", J. Phys.: Conf. Ser. **391**, 012168 (2012).

[H4] **K. Wohlfeld**, S. Nishimoto, M. W. Haverkort, J. van den Brink, "Microscopic origin of spin-orbital separation in Sr_2CuO_3", Physical Review B **88**, 195138 (2013).

[H5] V. Bisogni, **K. Wohlfeld**, S. Nishimoto,C. Monney, J. Trinckauf, K.J. Zhou, R. Kraus, K. Koepernik, C. Sekar, V. Strocov, B. Buchner, T. Schmitt, J. van den Brink, J. Geck, "Orbital Control of Effective Dimensionality: From Spin-Orbital Fractionalization to Confinement in the Anisotropic Ladder System $CaCu_2O_3$", Physical Review Letters **114**, 096402 (2015).

[H6] C.-C. Chen, M. van Veenendaal, T. P. Devereaux, **K. Wohlfeld**, "Fractionalization, entanglement, and separation: understanding the collective excitations in a spin-orbital chain", Physical Review B **91**, 165102 (2015).

[H7] **K. Wohlfeld**, C.-C. Chen, M. van Veenendaal, T. P. Devereaux, "Spin chain in magnetic field: limitations of the large-N mean-field theory", Acta Physica Polonica A **127**, 201 (2015).

[H8] E. M. Plotnikova, M. Daghofer, J. van den Brink, **K. Wohlfeld**, "Jahn-Teller effect in systems with strong on-site spin-orbit coupling", Phys. Rev. Lett. **116**, 106401 (2016).

(c) Discussion of the scientific / artistic goal of the above mentioned articles and the results achieved, together with the discussion of their potential use

Preface:
Between Noninteracting Collective Excitations and a Highly Collective 'Quantum Soup'

'More is different' is a celebrated idea which was postulated by Philip Anderson in the early 1970s [1]. It summarises the notorious feature of condensed matter physics: when one puts together a macroscopic number of interacting particles (e.g. electrons, atoms, or molecules), then the resulting state of matter formed by these particles has completely different properties than its constituents. Probably the most famous implementation of that idea is the concept of *order and collective excitations*. It turns out that the ground states of a number of condensed matter systems show order while its low-lying excited states can be most easily understood in terms of noninteracting quasiparticles, the so-called collective excitations [2]. A well-known example of that concept is the 'standard' crystal. In this solid material its constituents form a periodic arrangement (crystal lattice) leading to an ordered ground state. At the same time the low-lying excited states of the crystal can be described in terms of collective vibrations of all atoms in a crystal – the phonons.

More exotic realisations of the concept of 'order and collective excitations' can be found in crystals with local and anomalously strong electron-electron interactions. Such strongly correlated electron systems are ubiquitous to several transition metal compounds (typically oxides or fluorides) with deep lattice potentials [3]. Although these compounds may exhibit very distinct characteristics, what they all have in common is that the well-known properties of a single electron, such as for instance the electric charge or the spin angular momentum, may need to be considered as forming separate 'entities' [2,4]. While this is another facet of the idea that 'more is different', this also means that the collective excitations supported by these systems may for instance solely carry the electron's spin angular momentum – but no charge.

A nice example of such physics can be found in one of the most-studied class of transition metal compounds – the undoped quasi-2D copper oxides (La_2CuO_4, $CaCuO_2$, etc.). Here the electron-electron interactions, as for instance modelled by the 2D square-lattice Hubbard Hamiltonian [5], are so strong that they tend to localize electrons on the copper ions leading to the Mott insulating ground state of such a system[1]. Nevertheless, still virtual electronic motions are allowed, leading to the spin exchange processes: the effective interaction solely between the spin degrees of freedom of the electron [2,4]. The latter one can be modelled by a spin-only Heisenberg-like Hamiltonian [3,7]. The (zero temperature) ground state of that model shows antiferromagnetic (AF) long range order and the low lying excited states can be well-described in terms of noninteracting bosonic quasiparticles (called magnons) [4]. It turns out that the theoretically calculated dispersion of these collective magnetic excitations very well agrees with the one that was measured experimentally [7–9].

The fact that the low lying excitations of the undoped copper oxides can be successfully described by an essentially noninteracting theory is very appealing. Unfortunately, in the field of correlated electron systems such a situation is not that common. This is for instance the case of the so-called 'high-Tc problem', i.e. the question of the origin of the high-temperature superconductivity observed upon hole- or electron-doping the (already-mentioned above) copper oxides [3,5]. Here the concept of 'order and collective excitations' seems to break down and, despite more than 30 years of intensive research, the nature of the ground state of this strongly interacting system is not understood. Using the words of Jan Zaanen [10] one can say that such a ground state "(...) is some form of highly collective 'quantum soup' exhibiting simple yet mysterious properties such as the 'local quantum criticality' (...)".

In this review, we intend to understand a problem that lies in between these two extreme cases. That is, on one hand, far simpler than understanding the nature of that highly collective 'quantum soup'. On the other, it is significantly more complex than a simple noninteracting theory of collective excitations. As will be shown below, on the way to understand the main problem posed in this review, which concerns the nature of the collective orbital excitations (also called orbitons, see Sec. I below) that could be observed in the transition metal compounds, we will need to tackle the problem of *a condensed matter system which supports collective excitations of different kinds that are interacting with each other*.

The review is organised as follows. Sec. I introduces the basic concepts and problems of the so-called 'orbital physics' which are needed to define the main problem that is discussed in this review – i.e. the propagation of an orbiton in an antiferromagnet (Sec. II). Next, we discuss the solution to that problem as obtained for a 'minimal' spin-orbital model (Secs. III-V). Sections VI-VIII show the solutions to that problem as found for more realistic models, which can describe the physics observed in several transition metal oxides. Finally, in Sec. IX we summarize the findings and give a short outlook at the possible future studies.

I. Introduction: What Are Orbitons and Where to Find Them?

[1] One should note that the Mott insulators can be split into two separate classes [6]: (i) Mott-Hubbard insulators, (ii) charge transfer insulators. The copper oxides that are studied in this review are charge transfer insulators [3].

Quite often it is only the electron's *spin* angular momentum that needs to be taken into account in the electronic description of a solid. The *orbital* angular momentum, associated with binding of an electron to the nucleus of one of the atoms forming the solid, is often neglected. This is typically the case of weak lattice potentials and some 'conventional' metals or band insulators. However, in the case of deep lattice potentials found in the transition metal compounds the electrons 'live' in the atomic-like wavefunctions carrying distinct orbital quantum numbers. To put it differently: the noninteracting Hamiltonian of these solids can be written in terms of the atomic-like wavefunctions that are eigenstates of the orbital angular momentum operator [11–13]. How does the nonzero orbital angular momentum of an electron may affect the many-body (correlated) physics present in these compounds? Let us illustrate that on a simple, and probably the most famous, example – $KCuF_3$:

At first sight this copper fluoride with a perovskite structure seems to be somewhat similar to the mentioned in the Preface quasi-2D copper oxides. In the ionic picture the nominal valence of the copper ion is 2+ in this compound which leads to the the commensurate filling of one hole in the $3d$ shell of the copper ion. This, together with the strong on-site electron-electron repulsion, might in principle lead to a very similar physics as the one found in the quasi-2D cuprates and already described above. One could think that the 3D version of the Hubbard model should be good enough in describing the low energy electronic properties of this solid. This could then lead to the charge localization in the Mott insulating state and an effective (3D) spin-only Heisenberg model with antiferromagnetic long range order and well-defined magnon excitations in low temperatures.

However, it turns out that in reality the physics of $KCuF_3$ is quite different. The culprit is the orbital degree of freedom or, more precisely, the so-called 'orbital degeneracy'. Unlike the quasi-2D cuprates which basically show tetragonal symmetry, the copper ions in $KCuF_3$ can be regarded as being in a cubic cage formed by the six nearest neighbor oxygen ions. Since the wave functions pointing toward fluorines have higher energy in comparison with those pointing between them, two of the lowest lying (in hole language) $3d$ orbitals are degenerate in this picture. These are the cubic harmonics $d_{x^2-y^2}$ and $d_{3z^2-r^2}$ (jointly called as the 'e_g orbitals'). Such degeneracy strongly modifies the many-body physics: while the charge is still localized as a result of strong electron-electron repulsion and commensurability, the virtual electronic motions are now permissible between electrons with different spin *and* orbital quantum number. Consequently, instead of a simple spin-only Heisenberg model, the effective low energy model (often called spin-orbital or Kugel-Khomskii) contains both spin and orbital degrees of freedom model Hamiltonian [12]] and takes the following form

$$\mathcal{H} = J \sum_{\langle \mathbf{i},\mathbf{j}\rangle ||\Gamma} \left(\mathbf{S_i}\cdot\mathbf{S_j} + A\right)\left(B\ T^z_{\mathbf{i}} T^z_{\mathbf{j}} + C\ T^x_{\mathbf{i}} T^x_{\mathbf{j}} + D_\alpha\ T^\alpha_{\mathbf{i}} + E\right), \tag{1}$$

where J is the spin-orbital exchange, A, B, C, D_α, E are constants of the model (which depend on the orbital hoppings and on the ratio of the Hund's exchange to the on-site Coulomb repulsion), and $\Gamma = a, b, c$ is a particular direction in the cubic lattice formed by copper ions, Crucially, $\mathbf{T_i}$ is a $T = 1/2$ orbital (pseudo)spin operator on site $\mathbf{i}$ which is a three component vector ($T^\alpha_{\mathbf{i}}$ where $\alpha = x, y, z$) and which takes care of the orbital degrees of freedom (the two eigenvalues of T^z_i correspond to one of the two e_g orbitals being occupied), cf. [12, 14] for further details. Note that the interaction between orbital degrees of freedom lacks the $SU(2)$ symmetry which is a consequence of the finite Hund's exchange and the distinct hopping elements between different orbitals. This situation is typical to several spin-orbital models [15].

Finding the ground state of the inherently interacting model (1) is a complex task. It is still a matter of active research [16–18], despite the 35 years that has passed since the seminal paper by Kugel and Khomskii [12]. Nevertheless, a relatively good insight into the problem can be obtained by firstly considering just one plane of this 3D model (which corresponds to the ab plane of $KCuF_3$) and by going to the orbital basis formed by the $d_{x^2-z^2}$ and the $d_{y^2-z^2}$ orbitals, i.e. without off-diagonal hoppings between orbitals in the ab plane. Then, a simple of the spin-orbital model (1) suggests that the ground state of that Hamiltonian should show alternating-orbital (AO) order in the ab plane [cf. Fig. 1(a)] and a concomitant spin ferromagnetic (FM) order[2]. On the other hand, a similar analysis for the c direction yields the same energy for the ferroorbital (FO) order and AO order, both accompanied by the AF order – hence two different types of orbital ordering are realized in $KCuF_3$, cf. Fig. 1(a). We should note that, although it is still not completely clear what the ground state of model (1) is and whether the Jahn-Teller effect may also play a significant role in stabilizing the observed orbital oder in $KCuF_3$ below $T \sim 800K$ [20–22], it is generally agreed that for the realistic values of the parameters the ground state of such a spin-orbital model supports long-range spin and orbital order [14, 17, 23].

As mentioned in the Preface, typically the onset of some type of order in the ground state of a condensed matter system leads to collective excitations from that ground state. Therefore, it should not come as a surprise that, as a

[2]While understanding in detail the origin of that type of spin and orbital order in this model is somewhat intricate, it is important to stress that such a tendency to the AO and FM order is triggered by the finite Hund's exchange that is inherently present in spin-orbital model Eq. (1), cf. Refs. [12, 19] and in particular Fig. 12 of Ref. [12].

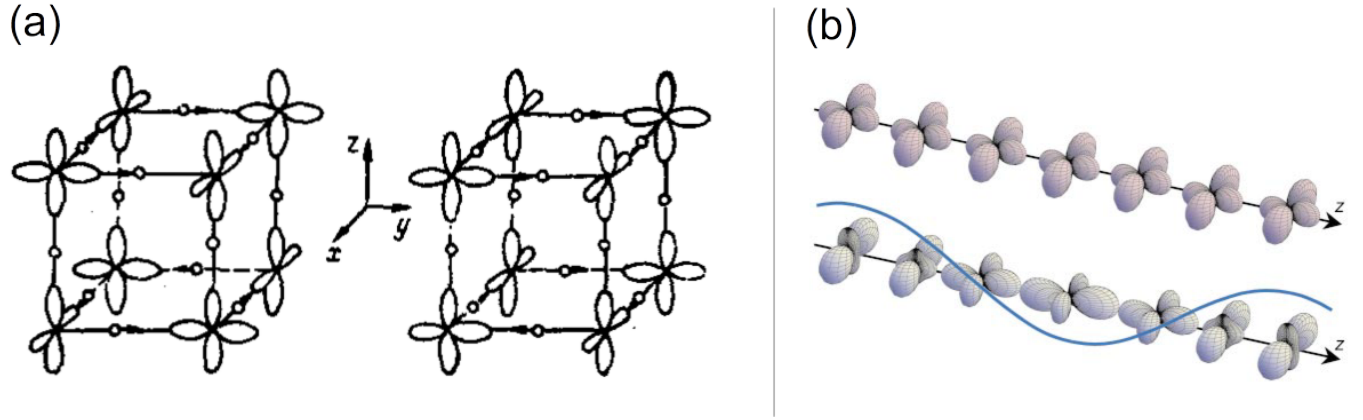

Figure 1: **Artist's view of the orbital order and of the orbiton** (a) Artist's view of the orbital order in $KCuF_3$ type as predicted by the the spin-orbital exchange model Eq. (1) with realistic parameters [AO order formed by the $d_{x^2-z^2}$ and the $d_{y^2-z^2}$ orbitals in the plane and either FO or AO order along c direction]; Left and right panels show two equivalent types of ordering (interestingly, both are observed in $KCuF_3$). (b) Artist's view of the propagation of the collective orbital excitation in an FO system; Top panel shows the FO ground state; Bottom panel show the orbital state with one orbiton at a particular momentum. [Panel (a) and caption adopted from Ref. [12]. Panel (b) and caption adopted from Ref. [24]]

result of the spin and orbital order present in the ground state of model (1), we should expect that collective spin and orbital excitations should appear here. Indeed, a mean-field decoupling of spins and orbitals in Eq. (1) predicts that those low energy excited states which carry solely the spin degree of freedom can indeed be described in terms of magnons [14]. This finding was confirmed by the inelastic neutron scattering experiment on $KCuF_3$ [25]. The fundamental question relates to the existence of the collective orbital interactions [26] – the so-called orbitons (this term was probably used for the first time in [27]), cf. Fig. 1(b). Indeed the mean-field analysis presented in [14] suggests that not only the orbitons but even joint spin-orbital collective excitations should be present in the model.

Unfortunately, so far the orbitons have not been observed experimentally in $KCuF_3$. What could be the reasons for that? It seems to us that the main problem lies on the experimental side. For years there had not been a reliable experimental probe to measure orbiton dispersion [28–30]. Even though neutrons couple to the orbital excitations [31], this cannot be easily realized experimentally [32] due to generally low energy transfers in the inelastic neutron scattering experiments. On the other hand, Raman scattering cannot transfer momentum to orbital excitations leading to controversies concerning the interpretation of the experimental spectra of $LaMnO_3$ – a 'sister'-compound to $KCuF_3$ [24, 31, 33]. Finally, while the resonant inelastic x-ray scattering (RIXS) [34] may seem to be the best probe of the orbitons [28, 29], so far it could not detect an orbiton[3] in the measured spectra of $KCuF_3$. The reason probably lies in the limiting energy resolution of RIXS: in order for the orbital excitation to be understood as having a collective nature (and thus be called an orbiton) we need to detect a finite orbiton dispersion. Since the magnitude of the orbiton dispersion is dictated by the size of the effective orbital exchange interaction, it usually is of the order of 10s of meV in the transition metal compounds – e.g. simple calculation of the orbiton bandwidth estimates it to be of the order of 10-20 meV in $KCuF_3$. Therefore, using the current RIXS resolution (ca. 55 meV at Cu L edge, cf. Ref. [9]) the orbiton cannot be unambigously detected in $KCuF_3$.

An even more disturbing fact is that basically till 2012 (cf. paper [H2] and below) the orbitons had not been unambiguously detected in any transition metal compound. First of all, as already mentioned above, the Raman scattering has not managed to detect orbitons in $LaMnO_3$, probably the most famous transition metal oxide with orbitally degenerate orbitals, as the earlier results [24] were rejected by a consecutive study [33]. While few other studies have shown the orbiton existence in an indirect way (e.g. through the so-called Davydov splittings [35] in Cr_2O_3, or in a pump-probe experiment in the doped manganite [36]), perhaps it was only in in the late 2000s that finally a small orbiton dispersion was indeed detected by RIXS on the titanates [37] – however, that signature was very weak as the dispersion was basically on the edge of the RIXS experimental resolution.

In this review, which is centered around the works published in the years 2011-2016, we suggest that the way to overcome the problem of finding the orbiton is to look at different systems: the transition metal oxides *without* orbital degeneracy in the ground state, i.e with relatively large crystal field splitting between orbital levels in the

[3]The experimental RIXS spectra taken at the Cu L edge of $KCuF_3$ do not show any signatures of orbitons (unpublished: C. Mazzoli, G. Ghiringhelli, K. Wohlfeld, and T. Schmitt).

ionic picture and, therefore, having (by definition) simple FO ground states (accompanied by the AF spin state due to the Goodenough-Kanamori rules [38, 39]). Naively, this might be a rather counterintuitive thing to do, since usually in this case one does not at all discuss the orbital degrees of freedom. However, one should bear in mind that this does not mean that the orbital degrees of freedom are simply irrelevant: it is just that the ground state description can be obtained without taking them into account. At the same time, the orbitals are important for the excited states in such compounds – and those can be accessed in an experiment (e.g. in RIXS). Crucially, the main advantage of choosing the FO-AF class of systems is as follows: as the exchange interaction is typically much larger in the FO and AF systems than in the AO and FM systems[4], there are higher chances of detecting the orbiton dispersion using the resolution of the currently available experimental techniques.

II. Subject of the Review: Propagation of an Orbiton in an Antiferromagnet

We have already stressed that the search for collective orbital excitations had turned out to be unsuccessful for several years. As already discussed, this might be due to the small spin-orbital exchange in systems with AO order. One of the ways to overcome this problem is to look for systems with the orbital FO and, as a result of the Goodenough-Kanamori rules [38, 39], spin AF ground states[5]. However, this requires understanding how such a collective orbital excitation can move in the AF state – which is the main subject of this review. We note already here that, due to the inherent entanglement of the spin and orbital degrees of freedom [41] in a wide class of spin-orbital models, this turns out to be a relatively complex problem. This statement is further supported by several works dedicated to the related problems [42–47] which suggest that the spin and orbital degrees of freedom cannot be decoupled on a mean-field level in a number of spin-orbital models. While in Sec. III immediately below we formulate and solve this question in the context of a 'minimal' spin-orbital model, we will discuss various aspects of this problem throughout the whole review.

III. 'Minimal' Spin-Orbital Model: Mapping onto a Single Hole Problem
This part describes the content of paper [H1] (partially)

We start by postulating the Hamiltonian of such a 'minimal' spin-orbital model. To this end, we require that: (i) to simplify the matters we concentrate on the lowest number of spin and orbital degrees of freedom per site that, however, still leads to a nontrivial solution; (ii) for the sake of the understanding we try to keep the model as close to the well-known Heisenberg model as possible; (iii) it has an AF ground state. This leads us to the following spin-orbital Hamiltonian with the Heisenberg [$SU(2)$–symmetric] interactions between both spin and orbital (pseudospin) degrees of freedom:

$$\mathcal{H} = 4J \sum_{\langle i,j \rangle} \Big(\mathbf{S}_i \cdot \mathbf{S}_j + \tfrac{1}{4} \Big) \Big(\mathbf{T}_i \cdot \mathbf{T}_j + \tfrac{1}{4} \Big) + E_z \sum_i T_i^z , \tag{2}$$

where $\mathbf{S}$ ($\mathbf{T}$) are the spin (pseudospin) operators that fulfill the $SU(2)$ algebra for $S = 1/2$ ($T = 1/2$) spins (pseudospins) and i and j are lattice sites and on each bond $\langle i,j \rangle$. Note that $T_i^z = (n_{ia} - n_{ib})$ where the operatore $n_{i\alpha}$ counts the number of electrons in orbital $\alpha = a, b$. The constant $J > 0$ gives the energy scale of the spin-orbital exchange (typically, but somewhat confusingly, called superexchange) and E_z the symmetry breaking field in the orbital sector. We note that the geometry and dimensions of the lattice needs not be defined at this stage.

It is relatively easy to verify that the above Hamiltonian fulfils the first two of 'our' requirements. As for the last one, which concerns the AF ground state, one needs to look a bit closer at the problem, for the ground state of the model obviously depends on the ratio of the model parameters E_z/J. In particular, once $E_z = 0$ the spin-orbital Hamiltonian has an $SU(4)$ symmetry, even higher than the combined $SU(2) \times SU(2)$ symmetries, which for instance in 1D results in the ground state given by the Bethe Ansatz and composite spin-orbital gapless excitations in addition to the separate spin and orbital ones (see, e.g., Ref. [48]). Therefore, the case $E_z = 0$ is not of interest here (see, however, Sec. V. below). On the other hand, once the crystal field is much larger than the spin-orbital exchange, $E_z \gg J$, then the ground state $|\psi\rangle = |\psi_S\rangle \otimes |\psi_O\rangle$ of Eq. (2) *decouples* into the 'spin' ($|\psi_S\rangle$) and 'orbital' ($|\psi_O\rangle$) sectors. This is because in this limit, in the 'orbital sector' the ground state of the above Hamiltonian is ferroorbital (FO): $|\psi_O\rangle = |\mathrm{FO}\rangle$ is a simple product state of single-site eigenstates of the T_i^z operator with the $-1/2$ eigenvalue on each site i, while all other orbital configurations are separated from this state by a gap $\propto E_z$. At the same time, the 'spin sector' is then described as an eigenstate of the spin-only Heisenberg Hamiltonian with an effective spin exchange interaction equal to $2J$, i.e. it is an AF Heisenberg system formed by spins in the

[4] This roughly follows from the following reasoning: (i) in contrast to the AO-FM systems which usually occur for orbitally degenerate ground states in the ionic picture, the FO-AF are systems usually stabilized in the presence of large crystal fields, (ii) such crystal fields are to a large extent due to strong hybridization between transition metal ion and its ligands, (iii) strong hybridization means large hopping elements and therefore (potentially) strong spin and orbital exchange interactions.

[5] One should stress that for the hypercubic lattices (that of interest here) the ground state of the $S = \frac{1}{2}$ AF Heisenberg spin subsystems can be classified as *ordered*: it is spontaneously broken and long-range-ordered on a 2D or 3D square lattice [4] and is 'algebraically' ordered [4, 40] in one dimension (1D; due to the slowly decreasing power-law spin-spin correlations). Naturally, using such a terminology does not mean that we will *not* consider below the important differences between the 1D and 2D or 3D cases.

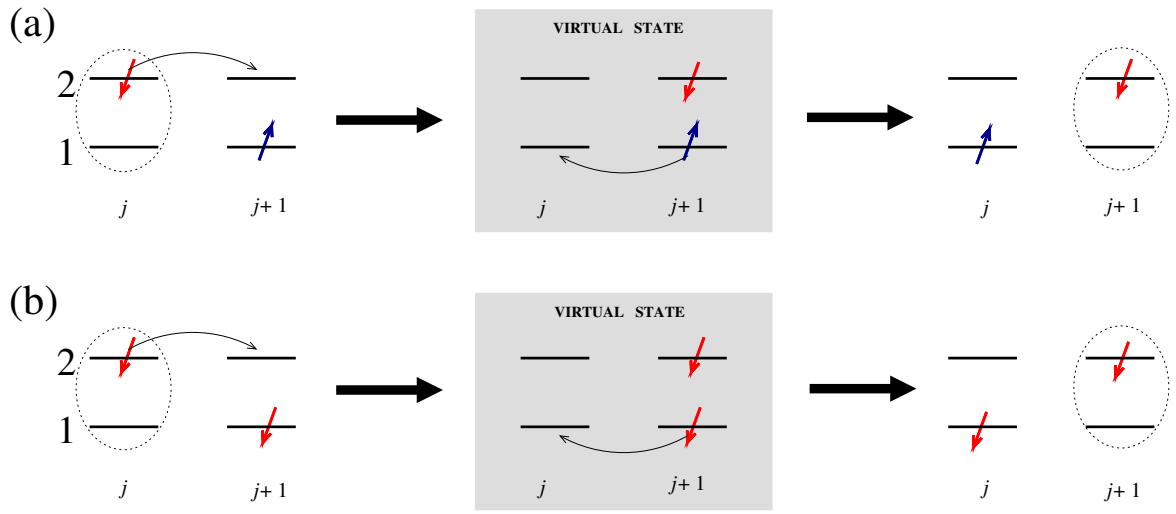

Figure 2: **Conservation of the spin on the excited orbital in the exchange process** Two spin-orbital exchange processes moving an electron in an excited orbital (indicated by oval) from site j to its neighbor $j+1$: (a) and (b) describe exchange process when spins along the bond are antiparallel or parallel, respectively, see text. The states in the grey middle panels are not part of the low-energy Hilbert space corresponding to (2). These virtual excitations within the full two-orbital *Hubbard* model illustrate the origin of those spin-orbital exchange interactions of Hamiltonian (2) that propagate the orbiton. Note that the spin of the excited electron is conserved, which is a crucial feature that enables the mapping of the orbital problem onto the effective t–J problem. [Figure and caption adopted from Fig. 1 of paper [H1]]

lower-energy orbital ($|\psi_S\rangle = |\mathrm{AF}\rangle$). While the precise form of the spin sector ground state depends on the choice of the lattice, for the most studied case of the hypercubic lattice and the $S = 1/2$ case it can basically be classified as 'ordered': it is spontaneously broken and long-range-ordered on a 2D or 3D square lattice [4] and is 'algebraically' ordered [40] in 1D (due to the slowly decreasing power-law spin-spin correlations). We note in passing that in this case the low energy excited states can typically be described in terms of noninteracting quasiparticles (spinons in 1D or magnons on 2D or 3D hypercubic lattices): the interactions between spinons (or magnons) are negligible provided their number in the AF is of the order O(1) and the system is infinite [49, 50].

Having understood that spin-orbital model (2) indeed has an AF ground state once $E_z \gg J$, we are now ready to formulate the above-mentioned main subject of this review in the context of this model. To this end, we define the following spectral function which describes the dynamics of the orbital excitation added to the AF ground state as

$$O(k,\omega) = \frac{1}{\pi} \lim_{\eta\to 0} \Im \left\langle \psi \left| T_k^- \frac{1}{\omega + E_\psi - \mathcal{H} - i\eta} T_k^+ \right| \psi \right\rangle , \tag{3}$$

where E_ψ is the energy of the ground state $|\psi_S\rangle$. The momentum-dependent orbital excitation is given by $T_k^+ = \sum_j \exp(ikj) T_j^\dagger$ [$T_k^- = (T_k^+)^\dagger$] with T_j^+ being the orbital raising operator which promotes an electron at site j from the occupied lower orbital to the empty higher one at the same site. Below we intend to calculate the orbiton spectral function and understand its properties. While that in principle can be done numerically (at least in the 1D case, see Sec. V below), here we follow a different approach. We perform an *exact mapping* of the orbital problem in question onto a well-known problem of a single hole in the AF ground state.

The crucial feature of the orbital problem, which permits such an exact mapping between these two problems, is related to the conservation of the spin on the excited orbital during its propagation, see Fig. 2(b). This peculiar conservation follows from the fact that irrespectively of the spin arrangement of the two nearest neighbor spins, the spin of the electron in the excited orbital does not change after the spin-orbital exchange process encoded in Hamiltonian (2). Consequently, the spin of the electron in the excited orbital can be understood as being a 'silent' degree of freedom and the electron in the excited orbital can be treated as a 'hole' in the AF ground state – with the sole difference that it propagates via a spin-orbital exchange $\propto J$ and not via the tight-binding hopping element $\propto t$.

Mathematically, the mapping proceeds as follows: (i) using the Jordan-Wigner transformation [51] we replace the spins (pseudospins) with spinons (pseudospinons), respectively; (ii) we observe that the pseudospinon-pseudospinon

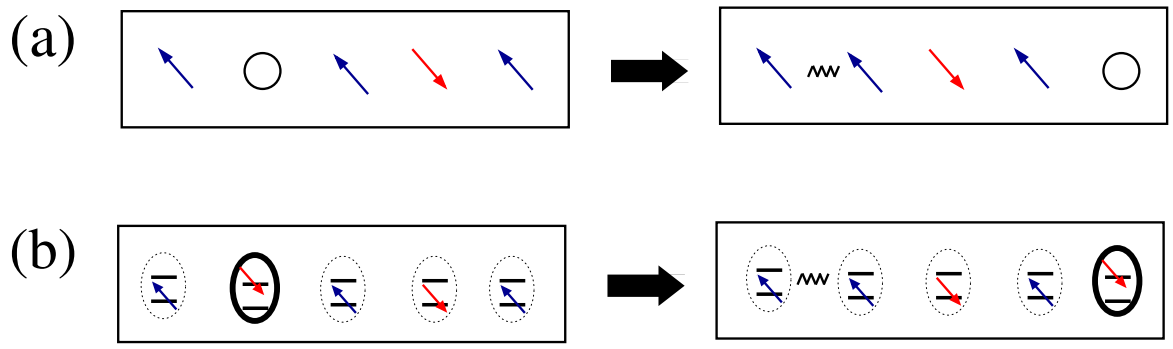

Figure 3: **Consequences of the mapping in 1D** (a) Schematic representation of the motion of a hole (circle) introduced in 1D AF (antiparallel arrows on nearest neighbors): although the first hop of the hole creates a spinon [wavy line, can further move (unshown) via spin exchange $\propto J$], all consecutive hops do not produce any extra spinons and the hole freely propagates as a 'holon' $\propto t$ giving rise to spin-charge separation in 1D. (b) Schematic representation of the motion of an orbital excitation (bold oval with the arrow in the upper bar) introduced in 1D AF: as a result of the mapping, the case is qualitatively similar to (a) and the orbital excitation moves as an 'orbiton', giving rise to spin-orbital separation. [Figure and caption adopted from Fig. 3 of paper [H1]]

terms vanish (due to the fact that there is just one pseudospinon in the whole bulk); (iii) we observe that (as a result of the above-mentioned conservation of the spin quantum number during the orbital propagation) one can introduce the constraint which requires that there can never be a pseudospinon and a spinon on the same site; (iv) we express all terms containing the pseudospinons in terms of the constrained fermions (the latter ones are fermions subject to the constraint of no double occupancies, cf. the t–J model problem [52,53]), cf. Ref. [54]; (v) we express all remaining terms containing spinons in terms of the $S = 1/2$ spins. It is interesting that the above procedure does not depend on the dimensionality of the problem (despite using the Jordan-Wigner transformation, which usually is better suited for the 1D problems). On the other hand, the mapping would no longer be exact if a spin-orbital Hamiltonian allowed for processes which do not conserve the spin quantum number during the orbital propagation (cf. Sec. VI below).

Altogether, we arrive at the following conclusion: It turns out that one can exactly map the problem of a single orbital excitation in the AF and FO ground state with its dynamics governed by the spin-orbital Hamiltonian [Eqs.(2-3)] onto a problem a single hole in the AF with the dynamics governed by the appropriate t–J model:

$$A(k,\omega)=\frac{1}{\pi}\lim_{\eta\to 0}\Im\left\langle\tilde{\psi}\left|\tilde{p}^{\dagger}_{k\uparrow}\frac{1}{\omega+E_{\tilde{\psi}}-\tilde{\mathcal{H}}-E_z-i\eta}\tilde{p}_{k\uparrow}\right|\tilde{\psi}\right\rangle. \tag{4}$$

Here $|\tilde{\psi}\rangle$ ($E_{\tilde{\psi}}$) is the ground state (energy of the ground state) of the undoped t–J model with the Hamiltonian given by

$$\tilde{\mathcal{H}}=-t\sum_{\langle i,j\rangle,\sigma}\left(\tilde{p}^{\dagger}_{i\sigma}\tilde{p}_{j\sigma}+h.c.\right)+2J\sum_{\langle i,j\rangle}\left(\mathbf{S}_i\cdot\mathbf{S}_j+\frac{1}{4}\tilde{n}_i\tilde{n}_j\right), \tag{5}$$

where $\tilde{p}_{j\sigma}$ act in the restricted Hilbert space without double occupancies, $\tilde{n}_j=\sum_\sigma \tilde{n}_{jp\sigma}$, and the hopping parameter t is defined as $t = J$.

IV. 'Minimal' Spin-Orbital Model: Consequences of the Mapping

This part describes the content of paper [H1] (partially) and [H3] (partially)

Probably the most obvious advantage of the mapping lies in the reduction of the orbital problem to the one with fewer degrees of freedom. This, *inter alia*, means that the numerical solution of the problem can be performed on larger clusters. However, a more important by-product of the mapping is related to the understanding of the orbital spectral function – for we can now refer to a large number of older studies discussing the problem of a single hole in the AF ground state. For instance, restricting solely to the (most common in these model studies) hypercubic lattices, we infer that:

For the 1D case the t–J model studies [55–59] have predicted the onset of the so-called spin-charge separation [60, 61]: the hole introduced into the the undoped AF first creates a single magnetic domain wall (spinon) but then freely moves as a 'holon' in such a 1D AF. While the hole carries both the spin and charge quantum number,

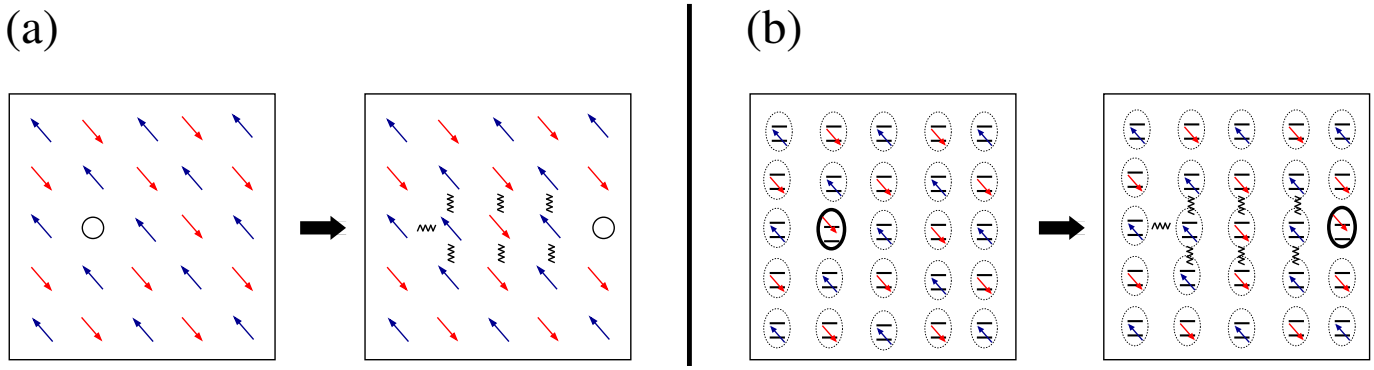

Figure 4: **Consequences of the mapping in 2D** (a) Schematic representation of the motion of a hole (circle) introduced in 2D AF (antiparallel arrows on nearest neighbors): the hole is subject to a string potential, for it creates spin defects (wavy lines) each time it makes a hop in a Neel-ordered 2D AF ground state [it can become mobile solely due to the existence of the spin fluctuations which can heal these defects (unshown)]. (b) Schematic representation of the motion of an orbital excitation (bold oval with the arrow in the upper bar) introduced in 2D AF: as a result of the mapping, the case is qualitatively similar to (a) and the orbital excitation is subject to a string potential in a 2D AF. [Figure and caption adopted from Fig. 2 of paper [H3]]

the spinon (holon) solely carries the spin (charge) quantum number and one can talk of a spin-charge separation, cf. Fig 3(a). For the orbital case this translates into the orbital excitation, which originally carries both orbital and spin degree of freedom, splitting into the spinon and 'pure' orbiton collective excitations, cf. Fig 3(b). We call this phenomenon a 'spin-orbital separation'.

On the other hand, a different situation occurs for the 2D or 3D lattice. In the simplest picture, the hole added to such an AF state introduces magnetic defects each time it makes a hop in a Neel-ordered 2D or 3D AF ground state [62]. As a result the hole is confined in a string-potential, cf. Fig 4(a). However, a more realistic picture reveals that these defects can be healed by quantum spin fluctuations $\propto J$ that the hole can become mobile – albeit not on a scale of the original free hopping $\propto t$ but rather $\propto J$ [63, 64]. In the literature the latter situation is often referred to as a 'spin polaron' [64], since the hole becomes mobile by dressing with the collective magnetic excitations (magnons). Due to the mapping, a similar conclusion can be formulated for the orbiton: the orbiton in a 2D / 3D AF is subject to a string potential [cf. Fig 4(b)] and can become mobile solely by dressing with magnons.

V. 'Minimal' Spin-Orbital model: Compatibility of the Mapping Results with Other Approaches
This part describes the content of papers [H6] and [H7] with a reference to [H1]

We mentioned above that the mapping is exact. Nevertheless, to fully understand the physics behind the mapping, it is necessary to compare the orbital spectral function calculated using the mapping against the exact numerical solutions as well as other available quasi-analytical solutions. *Below we concentrate solely on 1D, since such a comparison is basically only feasible in 1D*: the numerically exact result experience large finite size effects, while the combination of cluster perturbation theory and exact diagonalization, that can be well-implemented in 1D (see below), fails in 2D [65]. Moreover, there is also a well-known lack of reliable quasi-analytical approaches above 1D: (i) Bethe Ansatz is developed solely for the 1D spin-orbital model [66–69], (ii) the large-N mean-field approach [70–72] cannot be used for symmetry broken states that can be stabilized in two or higher dimensions, and (iii) the usual mean-field decoupling of spins and orbital [41] followed by a linear spin and / or orbital wave approach already does not lead to reasonable results in 1D.

We start by showing the orbital spectral function calculated using the mapping for the case with $E_z = 20J$ (i.e. the requirement $E_z \gg J$ is easily fulfilled), see Fig. 5(T). The spectrum, calculated using Lanczos exact diagonalization method on a 28-site chain, is not formed by one single branch but instead it consists of multiple peaks (expected to merge into incoherent spectrum in the thermodynamic limit) with a dominant feature at the lower edge of the spectrum. Using spin-charge separation Ansatz [56, 57], adopted to the unusual case when the spin exchange is larger than the hopping, we observe that the bottom of the orbital spectral function is given by the dispersion relation $\omega \approx E_z - 2t \sin|k|$ and is if a pure orbiton character. On the other hand the continuum above that edge reflects both spinon and orbiton excitations – except for the intermediate feature still well-visible within the continuum with the dispersion of the purely orbiton-character scaling as $\omega \approx E_z + 2t \sin|k|$.

We are now ready to compare the result obtained from the mapping with those that could be obtained using other approaches:

First, we compare the spectrum obtained using the mapping to the numerically exact solution of the original spin-orbital problem, i.e. Eqs. (2-3). It occurs that both calculations, obtained using the Lanczos exact diagonalization suplemented by cluster perturbation theory [73, 74] on a 16-site chain, give completely *identical* spectra, cf. Fig. 5(L)(f) which qualitatively shows the same spectrum as Fig. 5(T) (for a detailed comparison showing quantitative agreement cf. Fig. 6(a) in paper [H6]). This *a posteriori* justifies the fact that the mapping is exact.

Second, we discuss the orbital (and spin) spectral function (3) calculated using a mean-field decoupling between spin and orbital operators in model Eq. (2), cf. Ref. [41]. This method is relatively straightforward, since, as a result of the Holstein-Primakoff transformation and linear orbital wave approximation that is employed to the decoupled orbital part of the spin-orbital Hamiltonian, it leads to a quadratic Hamiltonian which can be solved analytically. Such a decoupling was shown in the past to be relatively successful in correctly reproducing the ground and excited states of several spin-orbital models – e.g. an analogous procedure was also performed for the magnons with FM and AO order in $LaMnO_3$ and $KCuF_3$ and gave a good agreement with experiment [25, 75]. Applying this procedure to the Hamiltonian (2) in the limit of $E_z \gg J$ leads to the orbital spectral function consisting of a single mode with a dispersion relation $\omega_{OW}(k) = E_z - \frac{1}{2} z J_{\rm OW}(1-\gamma_k)$. Here z is the coordination number, γ_k is the lattice structure factor, and the effective orbital exchange constant $J_{\rm OW} = 4J\langle\psi_S|\mathbf{S}_i\cdot\mathbf{S}_j + \frac{1}{4}|\psi_S\rangle$. Thus, in contrast to the exact case, the orbital excitation on the mean-field level is a quasiparticle with a cosine-like dispersion with period 2π, cf. the solid violet line in Fig. 5(T). This means that such a mean-field decoupling fails completely in the present case.

Third, we may wish to compare the results from the mapping with those based on the analytically exact solution following the Bethe Ansatz [66, 68, 76]. The latter predicts that a spin and orbital dynamical structure factor of model Eq. (2) should be built out of three 'flavorons' – the collective excitations of this model, each carrying both spin and orbital quantum number but (naturally) no charge. While this solution is exact and valid for *any* value of the crystal field E_z in model Eq. (2), not only understanding the nature of 'flavorons' is a complex task but also it is extremely difficult to obtain the spectral information from any type of the Bethe Ansatz solution [77]. Therefore, we turn our attention to *another* mean-field decoupling, that is based on the so-called mean-field large-N theory of constrained fermions [70–72], can be used here and gives reasonable results. The method is based on firstly expressing the spin and orbital operators in Eq. (2) in terms of the so-called constrained fermions $f^\dagger_{i\alpha\sigma}$, each carrying both orbital $\alpha = a, b$ and spin σ degree of freedom and subject to the constraint $\sum_{\alpha\sigma} f^\dagger_{i,\alpha\sigma} f_{i,\alpha\sigma} = 1$, and then performing a mean-field decoupling of the obtained in this way interacting Hamiltonian. The latter decoupling is done in such a way that it preserves the $SU(4)$ symmetry of the interactions between spins and orbitals (see [H6] for more details) and therefore it *may* give qualitatively correct results for systems without the spontaneously broken $SU(4)$ symmetry in their ground states [70–72]. The resulting mean-field Hamiltonian $\mathcal{H}_{\rm MF}$ reads

$$\mathcal{H}_{\rm MF} = \sum_{k,\sigma} \left(\varepsilon_{ka} f^\dagger_{ka\sigma} f_{ka\sigma} + \varepsilon_{kb} f^\dagger_{kb\sigma} f_{kb\sigma} \right), \tag{6}$$

where $\varepsilon_{ka/b} = -4\sqrt{2}J\cos(\delta_k)\cos(k)/\pi \mp E_z/2$, with $\delta_k = \arcsin[E_z\pi/(4J)]/2$ when $E_z < 4J/\pi$, and $\delta_k = \pi/4$ when $E_z \geq 4J/\pi$. The crucial point here is that this mean-field Hamiltonian represents two doubly degenerate fermionic bands with their energies $\varepsilon_{ka/b}$ separated by E_z. Due to the constraint of one fermion per site, the bands are filled up to the respective Fermi momenta: $\pm k_F \mp \delta_k$ and $\pm k_F \pm \delta_k$, where $k_F = \pi/4$ is the Fermi momentum at $E_z = 0$. Note that for $E_z = 0$ the fermionic bands are four times degenerate and quarter-filled, for $0 < E_z < 4J/\pi$ such orbital degeneracy is gone but all bands are occupied, for $E_z < 4J/\pi$ two of the four fermionic bands are fully occupied and two are completely empty. This result qualitatively agrees with the one obtained using the Lanczos exact diagonalization of the full Hamiltonian Eq. (2) which shows that for $E_z = 0$ the ground state shows AF and AO correlations without any orbital polarization, for $0 < E_z \lesssim 1.38J$ the ground state is AF and orbitals are partially polarized, and for $1.38J \lesssim E_z$ the ground state is AF and orbitals are fully polarized (FO order).

The main result here is that not only the ground state but also the low energy excited states can be qualitatively well-captured by the large-N mean-field Hamiltonian, Eq. (6). Moreover, this can be done for any value of the crystal field E_z. Figure 5(L) shows the spin dynamical structure factor defined as

$$S(k,\omega) = \frac{1}{\pi} \lim_{\eta\to 0} \Im \left\langle \psi \left| S^-_k \frac{1}{\omega + E_\psi - \mathcal{H} - i\eta} S^+_k \right| \psi \right\rangle, \tag{7}$$

and the orbital dynamical structure factor, $O(k,\omega)$ [see Eq. (3)], calculated using the Lanczos exact diagonalization and the cluster perturbation theory [73, 74] of the full Hamiltonian Eq. (2) for three distinct values of the crystal field E_z which correspond to three different regimes of the orbital polarization in the ground state. This result is compared to the compact supports[6] of the spin and orbital spectra calculated using the mean-field Hamiltonian

[6] As the mean-field approach cannot account for the spectral intensity [78] we only concentrate on the compact support.

(T)

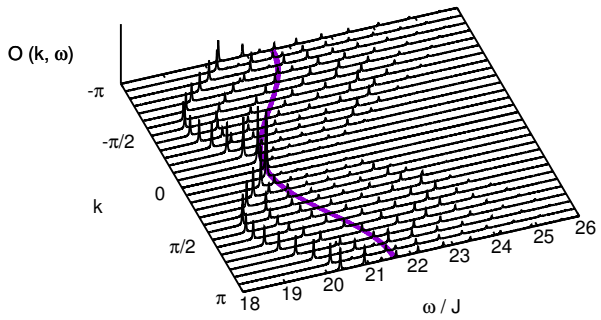

(L) (R)

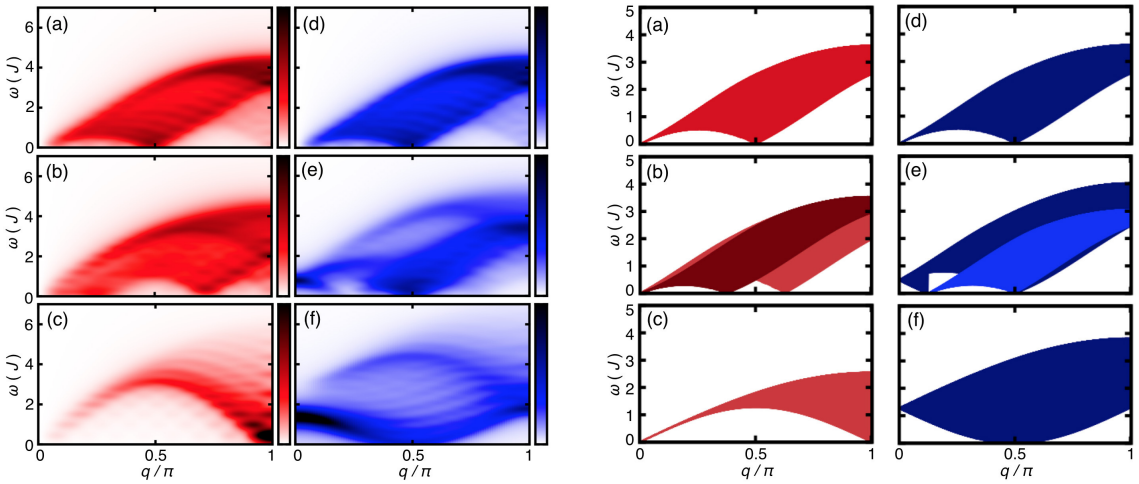

Figure 5: **Compatibility of the mapping results with other approaches** (T) Comparison of the result from the mapping with the one obtained using the mean-field decoupling of spins and orbitals: orbital dynamical structure factor, Eq. (3), obtained via the mapping onto the t–J model, Eq. (4), evaluated using Lanczos exact diagonalization on a 28 site chain; a broadening $\eta = 0.06J$ and $E_z = 20J$; the thick line shows result obtained in a mean-field and linear orbital wave approach, see text. (L) Result from the exact diagonalization on a 16 site chain supplemented by the cluster perturbation theory: spin [(a)-(c)] and orbital [(d)-(f)] dynamical structure factor defined as in Eq. (7) and (3), respectively, at various E_z; top panels: $E_z = 0$, i.e. no orbital polarization; middle panels: $E_z \approx 0.83J$ leading to half polarized orbitals; bottom panels: $E_z \approx 1.38J$ leading to fully polarized orbitals; see [H6] for more details. (R) Result from the mean-field large-N theory of constrained fermions: compact support for spin [(a)-(c)] and orbital [(d)-(f)] spectra obtained by mean-field large-N theory of constrained fermions at various E_z; top panels: $E_z = 0$, i.e. no orbital polarization; middle panels: $E_z \approx 0.7\frac{4J}{\pi}$ leading to half polarized orbitals; bottom panels: $E_z = \frac{4J}{\pi}$ leading to fully polarized orbitals; see [H6] for more details. [Panel (T) and caption adopted from Fig. 2 of paper [H1]; note a different definition of the spin exchange J used in the review and in paper [H1] resulting in different energy scales in these manuscripts; panels (L) and (R) adopted from Fig. 4 and 5 of paper [H6]; q on the OX axis of panels (L) and (R) denotes the momentum of the excitation (that is defined as k in the main text)].

Eq. (6), see Fig. 5(R). The mean-field results agree well with the numerical simulations, for they can reproduce the shift in momentum of the zero-energy modes with the crystal field E_z as well as the overall bandwidths for the spin and orbital dynamical structure factors. On a qualitative level, the only discrepancy between numerics and the mean-field approach is related to the missing low-intensity branch in the mean-field spectra: that originates from the so-called ω flavoron [76] in the Bethe Ansatz solution of the $SU(4)$ symmetric model and would involve four constrained fermions, which cannot be captured in the mean-field theory.

According to the large-N mean-field approach, the excited states of the spin-orbital model Eq. (2) can be described in terms of noninteracting quasiparticles – the constrained fermions $f^{\dagger}_{k\alpha\sigma}$ where k here is the (crystal) momentum. Since each of such momentum eigenstates carries both spin and orbital quantum numbers, therefore the spin and orbital quantum number is *entangled* on each site, in a somewhat similar way as for the spin-orbital wave discussed in Ref. [79]. While such a result agrees with the general notion on the nature of collective excitations based on the Bethe Ansatz [66,68,76] and the numerical studies [69,79–81] mostly done for the $E_z = 0$ case, it stays in contrast with the result from the mapping onto the t–J model that suggests the spin-orbital *separation* when E_z is large enough to fully polarize the orbital ground state. How to reconcile that discrepancy? It turns out that the origin of this inconsistency lies in different definitions of the spin quantum number in these two approaches. Whereas in the large-N mean-field approach electrons in both lower and upper orbitals carry spin and orbital quantum numbers, in the studies involving the mapping onto an effective t–J model electrons in the lower (upper) orbital carry solely spin (orbital) quantum numbers, respectively. We note that the latter peculiar choice of the spin and orbital basis is possible only when the mapping of the spin-orbital model (having four degrees of freedom per site) to the t–J model (having three degrees of freedom per site) is allowed in a ground state with fully polarized orbitals.

Irrespectively of the value of the crystal field E_z, in the mean-field picture the spin and orbital spectra could be understood as originating in the 'particle-hole' excitations of the noninteracting constrained fermions $f^{\dagger}_{k\alpha\sigma}$ across the Fermi level. Thus, both spin and orbital excitations are always *fractional*, since the original single spin or orbital flip (as measured in the spin or orbital structure factor) splits into the independent constrained fermions, each carrying both a fraction of the quantum number of an electron and a fraction of the quantum number associated with a single spin or orbital flip. For instance, an orbital-flip excitation in $O(k,\omega)$, which means changing the orbital quantum number by $\Delta T^z = 1$, fractionalizes into two fermions: one carrying $(S^z = \pm 1/2, T^z = 1/2)$ quantum numbers, the other one carrying $(S^z = \pm 1/2, T^z = -1/2)$ quantum numbers, but (unlike electrons) both being chargeless.

Interestingly, the latter situation stays in contrast with the one encountered for the single spin chain in the magnetic field, see [H7]. In principle, also for this case one could employ the large-N mean-field theory. Unfortunately, this approach only works for spin chains in weak and moderate magnetic field. In this case the spin dynamical structure factor calculated numerically and using this mean-field approach qualitatively agree. Nevertheless, the quantitative agreement between these two approaches is worse than in the spin-orbital case. Moreover, the mean-field bands cannot accommodate more than 50% polarized spins and the large-N mean-field theory fails completely once the magnetic field is strong enough to polarize more than half of the spins in the ground state. Most importantly, however, the large-N mean-field approach cannot explain the excitations above the critical magnetic field that fully polarizes the ground state and turns it into a ferromagnet with no longer fractional excitations (the low lying excited states can be well-described in terms $S = 1$ quasiparticles – magnons). This means that the above mean-field theory works better for the spin-orbital model with the $SU(4)$ exchange interaction than for the $SU(2)$ spin chain and that the spin chain in external magnetic field can, in this context, be regarded as more complex than a spin-orbital chain in a magnetic or crystal field. This is because the mean-field approximation for SU(N) antiferromagnets gradually improves as N becomes larger [4, 72] and becomes exact for SU(N) models when $N \to \infty$.

VI. Extension: Orbiton in a Quasi-1D Copper Oxide and the Derivation of a Realistic Spin-Orbital Model

This part describes the content of papers [H2] and [H4]

A crucial test for most of the physical theories is their experimental verification. In the case of the above mentioned theory of the propagation of an orbiton in an antiferromagnet the situation is actually somewhat simpler. This is because 'our' theory was actually constructed owing to the access to the unpublished experimental results of J. Schlappa *et al.* in the end of 2009 and later published in paper [H2]. It turned out that the experimental data that was presented at that time to us [see Fig 6(a) and discussion below], and which contained the spectrum of orbital excitations as observed with RIXS at Cu L_3 edge in a quasi-1D cuprate (Sr_2CuO_3), had one very peculiar feature: large parts of the orbital spectrum seemed to be surprisingly similar to the photoemission spectrum of various quasi-1D cuprates [55, 58] that showed the onset of the spin-charge separation in 1D [60, 61]. It was this peculiar correspondence between these two seemingly different physical problems, that has inspired us in constructing the theory of the propagation of the orbiton in an antiferromagnet within the 'minimal' spin-orbital model – in particular the mapping between the spin-orbital and t–J model problem. Therefore, it should not come as a surprise that the presented below theoretical model, that on a qualitative level should be regarded as an extension to the 'minimal' spin-orbital model, will be able to successfully explain the experimental data and confirm that the suggested spin-orbital separation can indeed be realised in a strongly correlated crystal.

Let us now turn our attention to the understanding of that peculiar experimental RIXS data – the part of the RIXS spectrum taken at Cu L_3 edge on Sr_2CuO_3 that is of interest to us is shown in Fig. 6(a). In the past this

Mott insulating copper oxide had mostly been famous for an anomalously large spin exchange J, the extremely 1D character of its spin properties [82–84], and for the observation of spin-charge separation in the photoemission spectrum [85]. It turns out that these are not the sole interesting features of this compound – as Fig. 6(a) suggests there are three clear but peculiar characteristics of the RIXS spectrum of this compound: (i) a weakly dispersive peak situated at around 1.85 eV at $k = 0$, (ii) a strongly dispersive and pretty complex feature between 2.1 and 2.7 eV with the peak at $k = 0$ at ca. 2.36 eV, and (iii) a hardly dispersive peak at around 2.98 eV. How to interpret this spectrum?

First of all, according to the theory of the RIXS cross section [28–30, 34, 86] and in the widely-used fast collision approximation, one should think of RIXS at Cu L_3 edge as being directly sensitive to the orbital dynamical structure factor $O(k, \omega)$ in this energy range. Since in the simplest ionic picture the ground state orbital of the Cu^{2+} ion located in the tetragonal (D_{4h}) symmetry of the CuO_3 chains realized in Sr_2CuO_3 is the $3d_{x^2-y^2} \equiv x^2-y^2$ orbital that is occupied by a single hole[7], there should be four distinct orbital excitations (also called *dd* excitations) accessible within the $3d$ shell (due to the tetragonal crystal field the cubic harmonics basis is used): $3d_{xz} \equiv xz$, $3d_{yz} \equiv yz$, $3d_{xy} \equiv xy$ and $3d_{3z^2-r^2} \equiv 3z^2 - r^2$. As a result of that we obtain the following equation for the RIXS cross section at Cu L_3 edge in the interesting energy range:

$$I(k, \omega) = |L_{xy}(k)|^2 O_{xy}(k, \omega) + |L_{xz}(k)|^2 O_{xz}(k, \omega) + |L_{yz}(k)|^2 O_{yz}(k, \omega) + |L_{3z^2-r^2}(k)|^2 O_{3z^2-r^2}(k, \omega), \qquad (8)$$

where $O_\alpha(k, \omega)$ is the orbital dynamical structure factor related to a single excitation to one of the $3d$ orbitals ($\alpha = xz, yz, xy, 3z^2 - r^2$), and $L_\alpha(k)$ is the local RIXS form factor which follows from the dipole and fast collision approximation to the RIXS process, see paper [H4] for details. The dependence of these factors on the crystal momentum, explained in detail in paper [H4], follows from the fact that a change in the transferred momentum in the RIXS process leads to a change in the photon polarization vectors – and that influences the cross section, cf. Refs. [30, 34, 86].

A simple calculation, which takes into account not only the crystal field but also the covalency effects due to the hybridization of the electrons on the copper ion with the four nearest neighbor oxygen ions, suggests that the xy ($3z^2 - r^2$) is an excited orbital with lowest (highest) energy and that the energies of the xz and yz orbitals lie in between the other two orbitals and are degenerate. Such a structure was basically confirmed by the *ab-initio* quantum chemistry calculations. The obtained energies of the orbital excitations, $E_{xy} = 1.62$ eV, $E_{xz/yz} = 2.25/2.32$ eV, $E_{3z^2-r^2} = 2.66$ eV match, within a 15% error bar, the position of the three most intensive peaks found in the experimental spectrum at $k = 0$, cf. Fig. 6(a). Moreover, when the local RIXS form factor is taken into account, then the highest energy part of the RIXS spectrum can be surprisingly well reproduced using the 'local picture', i.e. assuming that the orbital excitations is dispersionless and that $O_{3z^2-r^2}(k, \omega) = \delta(\omega - E_{3z^2-r^2})$, cf. the highest energy part of the experimental and theoretical spectrum presented in Fig. 6(a) and (c). In fact, we have checked that, according to the DFT calculations, the hybridization of the $3z^2 - r^2$ orbital with the nearest neigbor oxygen orbitals is anomalously small in Sr_2CuO_3, i.e. it is much smaller than the simple Slater-Koster scheme would suggest [87]. This further confirms that the momentum-dependence of the intensity of the $3z^2 - r^2$ peak is solely due to the local RIXS form factor.

The main problem here concerns the calculation of the orbital dynamical structure factor for the xy and xz/yz orbital excitations, i.e. obtaining a model which could explain the onset of the weak dispersion of the xy orbital and the much stronger and more complex dispersion associated with the xz/yz orbital. Let us first speculate on the possible origin of the onset of the latter dispersion. We observe that lower branch seems to have a dominant π period component and the upper branch seems to have a rather particular shape which altogether leads to the onset of two 'oval'-like features in the RIXS spectrum between 2.1 and 2.7 eV. On a qualitative level this is very similar to the theoretical orbital spectrum calculated for the 'minimal' spin-orbital model, see Fig. 5(T). Encouraged by this positive results we derived and solved in paper [H4] a realistic spin-orbital model that could describe the propagation of both the xy and the xz/yz orbital excitation and is able to give a good quantitative agreement with the experiment. Here we summarize the crucial steps needed to obtain the orbital spectrum of that realistic spin-orbital model:

- Our starting point is the proper *charge transfer model* which, as already pointed long time ago by Zaanen, Sawatzky, and Allen [6], should correctly describe the low energy physics of the copper oxides. The crucial feature of this class of models is best understood in the hole language: it corresponds to the fact that in the copper oxides it costs less energy to put an extra hole on the unfilled oxygen $2p$ shell (charge transfer Δ) than on the single-occupied copper $x^2 - y^2$ orbital (Hubbard U). Therefore, the oxygen degrees of freedom cannot be as easily integrated out as in the case of the 'standard' correlated systems with the low energy physics happenning only on the transition metal ions. The basic form of this 1D model for the CuO_3 chains

[7] In what follows the hole language is used.

in Sr_2CuO_3, including the suggested values of its parameters, was put forward by R. Neudert *et al.* [88]. In papers [H2] and [H4] we extended this model, in order to include the copper xy and the xz as well as those oxygen $2p$ orbitals which, according to the Slater-Koster scheme [87], should strongly hybridize with these two $3d$ orbitals. Thus, in total, the model contains three $3d$ orbitals per copper ion and three $2p$ orbitals per oxygen ion ($2p_x \equiv p_x$, $2p_y \equiv p_y$, and $2p_z \equiv p_z$), see Eqs. (2-5) in paper [H4], and 18 model parameters. The values of the model parameters mostly follow Ref. [88] with a few of them taken from the in-house LDA calculations or estimated following Ref. [89]. We note that, as we choose that the CuO_3 chains lie along the x direction, we can safely assume that the yz orbital should be nondispersive, since the hopping from the yz orbital along the chain direction should be strongly suppressed [87]. Hence, we can write that $O_{yz}(k,\omega) = \delta(\omega - E_{yz})$.

- As both U and Δ are much larger than all the hopping elements (t_n) of the Hamiltonian we can hugely *simplify the charge transfer model by considering perturbation theory in* t_n/Δ *and* t_n/U.
- In the zeroth order in the perturbation theory in hoppings t_n of the charge transfer model and in the regime of one hole per copper site, the large Coulomb repulsion U and the charge transfer energy Δ cause Sr_2CuO_3 to be a Mott insulator. This is because, in the zeroth order approximation in the perturbation theory in hopping t_n and in the regime of one hole per copper site, there is one hole localized in the x^2-y^2 orbital at each copper site i.
- The second order perturbation theory[8] in the hoppings t_n leads to a relatively strong renormalization of the on-site energies of the orbital excitations due to the formation of the bonding and antibonding states between the copper orbital and its nearest neighbor oxygen orbitals. However, since in the final calculations the on-site energies of the xz and xy orbital excitations will anyway be taken from the *ab-initio* quantum chemistry calculations (see below), we can safely disregard this contribution.
- The most interesting contribution arises from the fourth order in the perturbation theory in hoppings t_n – these are the so-called superexchange processes in transition metal oxides [90]. This contribution defines the bulk part of the spin-orbital model and can be split into three distinct parts:
  - When only the ground state x^2-y^2 orbital is occupied by a single hole on two nearest neighbor copper sites – this leads to the following *spin* superexchange Hamiltonian:

$$\mathcal{H}_{\rm spin} = J(1+R)\sum_{\langle i,j\rangle}\mathcal{P}_{i,j}\left(\mathbf{S}_i\cdot\mathbf{S}_j - \frac{1}{4}\right), \tag{9}$$

    where $\mathbf{S}_i$ is the $S=1/2$ spin operator for spins on the copper site i, the projection operator $\mathcal{P}_{i,j}$ makes sure that there are no orbital excitations along the $\langle i,j\rangle$ bond, the spin exchange is defined as $J = \frac{4t_\sigma^4}{(\Delta_x+V_{dp})^2}\frac{1}{U}$, and $R = \frac{2U}{2\Delta_x+U_p}$ is the factor responsible for the onset of the superexchange processes on the oxygen ion. Here t_σ is the (renormalized due to the covalency effects, see paper [H4] for more details) hopping element between the x^2-y^2 orbital and the nearest neighbor p_x orbital in the CuO_3 chain, Δ_x is the charge transfer energy for putting a hole into the p_x orbital, V_{dp} the Coulomb repulsion between holes on the nearest neigbor copper and oxygen ions (as already defined U is the Hubbard repulsion on the copper ion). The value of the spin exchange calculated in this way ($J(1+R) \approx 0.24$eV) well agrees with the one obtained from inelastic neutron scattering experiment $J = 0.24$ eV [91] as well as with the presented here resonant inelastic x-ray scattering at Cu L_3 edge which gives $J \approx 0.25$ eV (unshown low energy part of the RIXS spectrum, see Fig. 3 of [H2]).
  - When one copper site has a hole in the copper xz orbital and its nearest neighbor copper site has the hole in the ground state x^2-y^2 orbital we obtain the following spin-orbital Hamiltonian:

$$\mathcal{H}_{xz} = \sum_{\langle i,j\rangle}(\mathbf{S}_i\cdot\mathbf{S}_j + A)\left[BT_i^zT_j^z + \frac{C}{2}\left(T_i^+T_j^- + T_i^-T_j^+\right) + D\right], \tag{10}$$

    where $\mathbf{T}_i$ is the $T=1/2$ orbital peudospin operator with T_i^z is equal to the difference between occupation on the x^2-y^2 and the xz orbital [$T_i^z = (n_{i,x^2-y^2} - n_{i,xz})/2$]. All parameters of the model are defined in detail in paper [H4]. Here we only concentrate on parameter $C = J_{xz}(R_1+R_2+r_1+r_2)$, as this is the crucial parameter, being responsible for the hopping of the orbital excitations between nearest neigbor copper sites. It turns out that this model parameter depends on the orbital exchange $J_{xz} = \frac{(2t_\pi\bar{t}_\sigma)^2}{(\Delta_z+V_{dp})(\Delta_x+V_{dp})}\frac{1}{U}$, and on the four factors (R_1, R_2, r_1, r_2) which arise due to four distinct superexchange processes – two from the low spin intermediate states with two holes on the oxygen or copper sites and

[8] Contributions from first and other odd orders of perturbation theory vanish for this model.

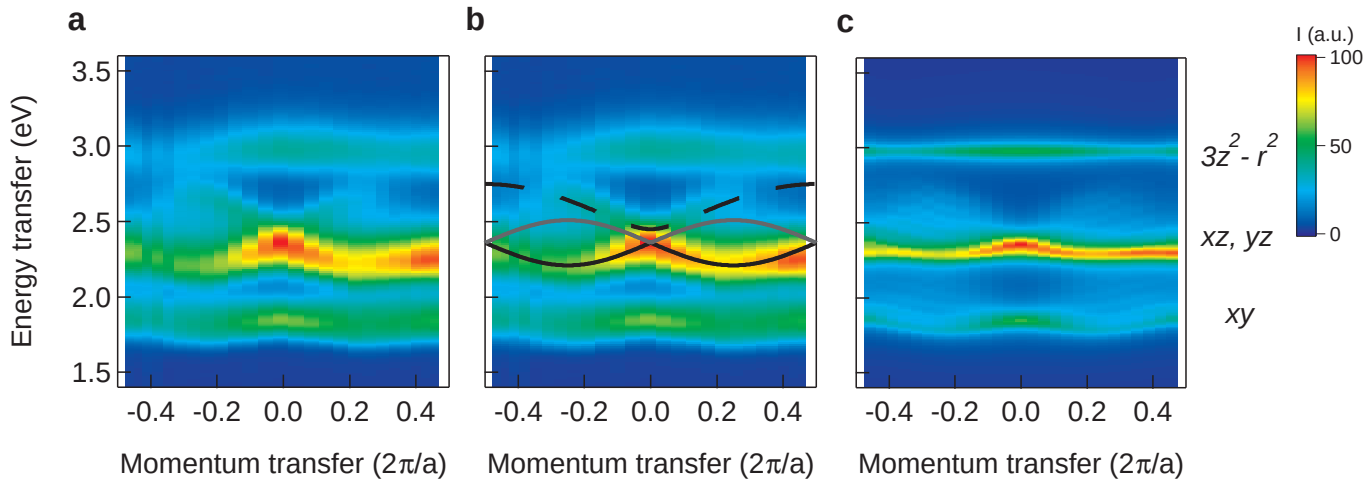

Figure 6: **Orbiton in a quasi-1D copper oxide in experiment and theory** (a) Experimental spectrum containing four orbital excitations [$3d_{xy}$, $3d_{xz}$, $3d_{yz}$, $3d_{3z^2-r^2}$, see legend on the right hand side of panel (c)] as obtained using resonant inelastic x-ray scattering at Cu L_3 edge of Sr_2CuO_3. Note that not all momenta (see white space in the spectrum close to $k \sim \pm\pi$) in the first Brillouin zone of Sr_2CuO_3 are reached for the photons with energy ~ 930 eV at Cu L_3 edge RIXS [34]. (b) Same as (a) but with the dispersion relations given by the spin-orbital separation Ansatz showing the dispersion of the pure orbiton (solid line) and the edge of the spinon-orbiton (dashed line) continuum of the $3d_{xz}$ orbital excitation (see text for more details). (c) Theoretical spectrum of orbital excitations as obtained using the spin-orbital model developed for Sr_2CuO_3 (see text for further details). [Panels and caption adopted from Fig. 4 of paper [H2]]

two from the high spin intermediate states with two holes on the oxygen or copper sites (they depend on the Hund's exchange and on the charge transfer energy, see [H4] for more details). Finally, t_π is the hopping element between the xz orbital and the nearest neighbor p_z orbital in the CuO_3 chain, Δ_z is the charge transfer energy for putting a hole into the p_z orbital.

– When one copper site has a hole in the copper xy orbital and its nearest neighbor copper site has the hole in the ground state x^2-y^2 orbital we obtain the following spin-orbital Hamiltonian:

$$\mathcal{H}_{xy} = \sum_{\langle i,j \rangle} (\mathbf{S}_i \cdot \mathbf{S}_j + A') \left[B' T'^z_i T'^z_j + \frac{C'}{2} \left(T'^+_i T'^-_j + T'^-_i T'^+_j \right) + D' \right], \tag{11}$$

where $\mathbf{T}'_i$ is the $T' = 1/2$ orbital peudospin operator with T'^z_i is equal to the difference between occupation on the x^2-y^2 and the xy orbital [$T'^z_i = (n_{i,x^2-y^2} - n_{i,xy})/2$]. Again all parameters of the model are defined in detail in paper [H4] and we only write down explicitly the parameter $C' = J_{xy}(R'_1+R'_2+r'_1+r'_2)$ with $J_{xy} = \frac{(2\bar{t}_\pi \bar{t}_\sigma)^2}{(\Delta_y+V_{dp})(\Delta_x+V_{dp})} \frac{1}{U}$, the four factors ($R'_1$, R'_2, r'_1, r'_2) again arising due to four distinct superexchange processes, and $\bar{t}_\pi$ being the (renormalized due to the covalency effects, see paper [H4] for more details) hopping element between the xy orbital and the nearest neighbor p_y orbital in the CuO_3 chain, Δ_y – the charge transfer energy for putting a hole into the p_y orbital.

- Having derived the relevant spin-orbital model, we are now ready to calculate the relevant orbital dynamical structure factor – for the single orbital excitation of the xz character

$$O_{xz}(k,\omega) = \frac{1}{\pi} \lim_{\eta \to 0} \Im \left\langle \psi \left| T^-_k \frac{1}{\omega + E_\psi - \mathcal{H}_{\rm spin} - \mathcal{H}_{xz} + i\eta} T^+_k \right| \psi \right\rangle, \tag{12}$$

as well as for the single orbital excitation of the xy character

$$O_{xy}(k,\omega) = \frac{1}{\pi} \lim_{\eta \to 0} \Im \left\langle \psi \left| T'^-_k \frac{1}{\omega + E_\psi - \mathcal{H}_{\rm spin} - \mathcal{H}_{xy} + i\eta} T'^+_k \right| \psi \right\rangle, \tag{13}$$

where in both cases $|\psi\rangle$ and E_ψ is the ground state and energy without any orbital excitations present, i.e. it is the ground state of $\mathcal{H}_{\rm spin}$.

- The above orbital structure factors are calculated using the mapping onto an effective t–J model, separately for each case (i.e. xz and xy orbital excitation). While the mapping basically proceeds as introduced in

Sec. III, there are two somewhat important differences here. First, the mapping is not exact, since in both cases the spin-orbital Hamiltonian allows for a propagation of the orbital excitation that does *not* conserve the spin quantum number of the electron in the excited orbital. Fortunately, that process, which is due to finite Hund's exchange J_H, has a relatively small contribution (it scales as $\propto J_H/U \sim 0.1 - 0.2$) and can be neglected. Second, also due to the finite Hund's exchange, the mapping leads to a small (10%) spin-dependence of the hoppings in the effective t–J model – which is also neglected.

Consequently, the problem of the orbital dynamical structure factor for the single orbital excitation of the xz character can be mapped onto the problem of a single hole in the effective t–J model, Eqs. (4-5) with its effective t and J parameters being replaced by: $t \to (3R_1+R_2+3r_1+r_2)/8J_{xz}$ and $J \to J(1+R)/2$. Similarly, the orbital dynamical structure factor for the xy orbital excitations can be calculated using the effective t–J model with $t \to (3R'_1 + R'_2 + 3r'_1 + r'_2)/8J_{xy}$ (and J as for the xz case). Moreover, in the definition of the spectral function, Eq. (4), we replace the on-site cost of creating a single orbital excitation, which was equal to the crystal field in the 'minimal' model, by its value as obtained from the *ab-initio* quantum chemistry calculations: $E_z \to E_{xz}$ and $E_z \to E_{xy}$, respectively for each case.

- The two problems of a single hole in the effective t–J models are solved using Lanczos exact diagonalization on a finite cluster.

The theoretical RIXS cross section, which follows Eq. (8) and *inter alia* includes the orbital dynamical structure factors for the xz and xy orbitals as explained above, is shown in Fig. 6(c). We observe that not only qualitative but also to a large extent quantitative agreement with the experimental spectra presented in Fig. 6(a). The sine-like shape of the experimentally observed dispersion relation of the xz and the xy orbitals, such as period π and minima at $\pm\pi/2$, is reproduced by the theoretical calculations. The same can also be said about the width and shape of the 'oval'-like bands above the dominant xz dispersive peak. Finally, also the relative intensities of the particular features of the theoretical and experimental spectra agree. The main discrepancy between the experiment and theory is related to the smaller dispersion in the theoretical calculations than in the experiment. This might for instance be due to the small but finite spin-orbit coupling in the $3d$ shell which would mix the xz and yz orbital excitations and could lead to a finite dispersion in the yz orbital channel.

The strong covalency effects lead to the effective hopping element t in the 1D t–J model being much larger for the xz orbiton than for the xy orbiton. Consequently the xz orbiton is more mobile than the xy orbiton and the characteristic features of the spin-orbital separation spectrum, well-known from Secs. III and IV, are much better visible for the xz orbiton than for the xy orbiton in the RIXS spectrum, cf. Fig 6(a), (c) with Fig. 5(T). This is even better visible, when the already used spin-charge separation Ansatz [56,57] is adopted to the effective t–J model for the xz orbtion ('spin-orbital separation Ansatz'), cf. Fig. 6(b). Here we observe that indeed the bottom of the experimental xz orbital spectral function is given by the dispersion relation $E_{xz} - 2t\sin|k|$ (where $t \to (3R_1 + R_2 + 3r_1 + r_2)/8J_{xz}$, see above) and is if a pure orbiton character, see the solid line in Fig. 6(b). The higher energy part of the xz spectral function is more complex: it contains another feature of the purely orbiton character with the dispersion given by $E_{xz} + 2t\sin|k|$ and an upper edge of the joint spinon-orbiton continuum that is given by $E_{xz} + \sqrt{4J^2 + 4t^2 + 8tJ\cos k}$ (where $J \to J(1 + R)/2$, see above). Altogether, this additional calculations further confirms that RIXS on Cu L_3 edge of Sr_2CuO_3 has observed the orbiton excitation.

Could other theoretical scenarios explain the experimental data equally well? Of course we could never exclude such a scenario entirely – however, a good agreement between theoretical modelling and experiments makes the task of finding such alternative frameworks rather challenging. In paper [H4] few of these are discussed: (i) the onset of the dispersion as a consequence of the momentum-dependence of the local RIXS form factors, (ii) a linear orbital wave approximation of the above-derived spin-orbital model, (iii) an observation of the spin-charge separation using RIXS, or (iv) the onset of the large dispersion following the large hopping elements between the oxygen $2p$ orbitals. It is suggested in [H4] that all of these theories cannot explain the experimental data equally well as the presented above spin-orbital model with the onset of the spin-orbital separation in this quasi-1D cuprate.

VII. Extension: Orbiton in a Ladder-like Copper Oxide and the Robustness of Spin-Orbital Separation

This part describes the content of paper [H5]

The experimentally observed spectrum of orbital excitations in the quasi-1D copper oxide, Sr_2CuO_3, can be very nicely understood using the 1D spin-orbital model. This *inter alia* lead to the first ever unambiguous observation of the orbiton dispersion and of the spin-orbital separation. One can wonder whether this is the only compound for which this novel physics can be observed. Below we give a very brief overview of the RIXS experiment on another copper oxide, $CaCu_2O_3$, and show that also that RIXS spectrum shows signatures of the orbiton dispersion and, despite its 'less-1D' structure, of the spin-orbital separation physics.

$CaCu_2O_3$ is a buckled two-leg spin ladder system that contains corner-sharing CuO_4 plaquettes [92, 93]. This compound is very similar to Sr_2CuO_3: due to strong correlations it is a Mott insulator with the localized holes on

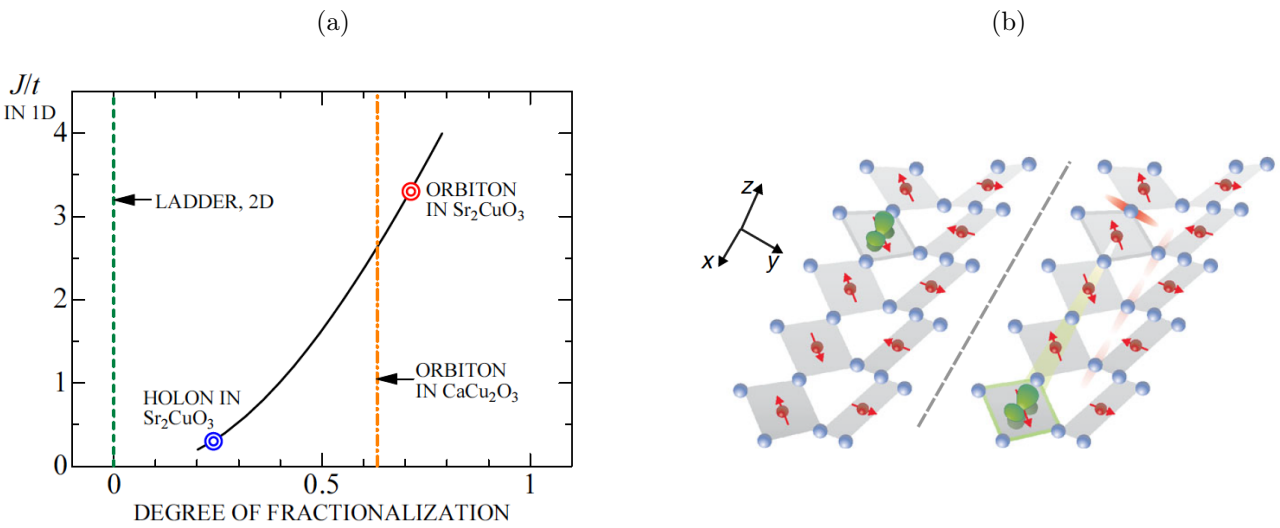

Figure 7: **Understanding spin-orbital separation in a ladder–like copper oxide** (a) Degree of fractionalization in various effective t–J models as obtained using the finite size scaled exact diagonalization: for the isotropic ladder t–J model (dashed line), for the anisotropic ladder t–J describing the spin-orbital separation in $CaCu_2O_3$ (dot dashed line), for the ideal 1D t–J model calculated as a function of J/t (solid line). $J/t \approx 0.4$ ($J/t \approx 3.3$) describes the spin-charge (spin-orbital) separation in Sr_2CuO_3. (b) Cartoon view of the orbiton propagation in the buckled two-leg ladder $CaCu_2O_3$: when the xz orbiton (marked in green) moves (compare left and right panels), it creates just one magnetic domain wall not only because interleg domain walls (light red) can be neglected (due to very weak spin interaction along the rung) but also because it can move *solely* along one of the legs of the ladders (due to the directional hopping of the xz orbital). [Panels and caption adopted from Fig. 4 and Fig. 1 of paper [H5]]

Cu^{2+} ions in the $x^2 - y^2$ orbitals. The superexchange processes are also allowed in this compound. They lead to the strong, though around twice smaller than in Sr_2CuO_3, Heisenberg-like spin interaction between the $S = 1/2$ spins of the localised holes along the leg direction of the ladder. Moreover, due to the buckling of the ladders leading to the onset of weak ferromagnetic exchange processes, the spin interaction across the rung of the ladder is relatively weak (10 times weaker than along the rung) which makes this ladder compound 'more 1D' and closer to Sr_2CuO_3 than one would naively expect judging from the ladder-like coordination of the copper and oxygen atoms in its crystal structure [93].

The RIXS experiment, that was performed on the Cu L_3 edge of $CaCu_2O_3$, reveals a relatively similar spectrum of the orbital excitations as in the case of Sr_2CuO_3, see Fig. 2 and 3 of paper [H5]. Again there are at least three well-distinguishable peaks between ca. 1.5 and 2.5 eV energy range. By comparing their energies to the quantum chemistry *ab-initio* calculations [94] one can easily assign the peaks lowest (highest) in energy to the xy ($3z^2 - r^2$) orbital excitation. These turn out to be nondispersive, for a theoretical RIXS cross section which assumes purely local orbital excitations well describes that part of the experimental spectrum. On the other hand, the part of the RIXS spectrum which is associated with the xz/yz orbital excitation seems to show nonnegligible dispersion relation.

Can one reproduce the observed experimental behaviour, in particular the nondispersive character of the xy orbital excitation and the dispersion of the xz/yz orbital excitation, with a theoretical model? It turns out that this indeed *is* possible (see excellent agreement between theory and experiment shown in Fig. 3 of paper [H5]) and that one can do that following similar steps as proposed in Sec. VI for Sr_2CuO_3. In order not to dive too much into the details below we merely mention the main differences between these two cases:

- The charge transfer model is defined on a (buckled) two-leg ladder instead of the 1D chain. As obtaining the correct values of the hopping parameters in this buckled system is a crucial step in modelling the orbital spectrum of this compound, the hopping parameters of its tight-binding part are obtained from the in-house DFT calculations (FPLO code, cf. Ref. [95]). We note in passing that the other parameters of the model follow (as for Sr_2CuO_3) Ref. [88], since we do not expect the Hubbard U or the charge transfer energies to substantially changed between different copper oxides.
- Consequently, the spin model, obtained from charge transfer model in the fourth order perturbation theory,

is defined on a two-leg ladder and reads:

$$\mathcal{H}_{\rm spin} = J_{\rm rung} \sum_{\langle \mathbf{i},\mathbf{j}\rangle || {\rm rung}} \mathcal{P}_{\mathbf{i},\mathbf{j}} \left(\mathbf{S}_\mathbf{i} \cdot \mathbf{S}_\mathbf{j} - \frac{1}{4} \right) + J_{\rm leg} \sum_{\langle \mathbf{i},\mathbf{j}\rangle || {\rm leg}} \mathcal{P}_{\mathbf{i},\mathbf{j}} \left(\mathbf{S}_\mathbf{i} \cdot \mathbf{S}_\mathbf{j} - \frac{1}{4} \right), \tag{14}$$

where $\mathcal{P}_{\mathbf{i},\mathbf{j}}$ is defined as in Eq. (9) and due to the buckling the model is very anisotropic, i.e. $J_{\rm rung} \approx J_{\rm leg}/12$, cf. Refs [25, 93].

- An important difference arises when deriving the spin-orbital model for the xy orbital excitation. It turns out that the hopping along the leg of the ladder is blocked due to a rather peculiar interplay of the Pauli principle and a covalency effect following the strong interladder hopping between the p_y oxygen orbital in the leg and the $x^2 - y^2$ copper orbital in the neighboring ladder. As explained in detail in paper [H5] the coherent travel of the xy orbital along the leg is suppressed and therefore we can safely model using it a purely local picture (the motion along the rung is not resolved in the RIXS experiment, since there is no transferred momentum along the rung in the chosen geometry of the RIXS experiment).
- Although for different reasons, the situation for the xz orbital excitation is somewhat opposite to the xy case: the spin-orbital superexchange processes are allowed along the leg (and no covalency and Pauli principle effects can hinder its motion along the leg), the hopping along the rung vanishes completely due to the 'one-dimensional' character of the hopping from the xz orbital [cf. Fig. 7(b)]. As a result we obtain the purely 1D spin-orbital Hamiltonian for the xz orbital orbital excitation:

$$\mathcal{H}_{xz} = \sum_{\langle \mathbf{i},\mathbf{j}\rangle || {\rm leg}} (\mathbf{S}_\mathbf{i} \cdot \mathbf{S}_\mathbf{j} + A) \left[B T^z_\mathbf{i} T^z_\mathbf{j} + \frac{C}{2} \left(T^+_\mathbf{i} T^-_\mathbf{j} + T^-_\mathbf{i} T^+_\mathbf{j} \right) + D \right], \tag{15}$$

where (naturally) all the parameters of the model are differ quantitatively w.r.t. the Sr_2CuO_3 case.

The effective t–J model, which follows through the mapping from the above model Eqs. (14-15) and describes the propagation of the xz orbiton in $CaCu_2O_3$ is not strictly 1D: although the hopping of a hole has a strictly 1D character, there is a small but finite spin interaction along the ladder rungs, see Eq. 14. Nevertheless, the orbiton spectrum calculated from this model using exact diagonalization on a 14×2 ladder cluster seems to be very similar to the one of the completely 1D model and a spin-orbital separation Ansatz seems to well-describe the spectrum, cf. Fig. 3 of paper [H5]. On the other hand, the analysis of the magnetic spectrum of $CaCu_2O_3$ suggests that for the energy scale $E \ll J_{rung}$ spinons are *not* the 'correct' collective excitations [92].

In order to establish whether the spin-orbital separation really takes place in this model on the here relevant energy scale, we define the so-called 'degree of fractionalization' as the ratio between the correlation $\lambda(r)$ at $r = \infty$ and $r = 1$ with λ defined as the correlation between the orbital (or charge in the case of spin-charge separation) degree of freedom at site $i = 1$ and the spin at site $i + r$. This quantity expresses how well the spinon and the orbiton (or holon) are separated from each other and it ranges from 0 (not separated) to 1 (fully separated). Numerically the degree of fractionalization is calculated using the finite size scaling, which was needed in order to estimate the value of the correlations at infinite distance. The results, obtained for various models and shown in Fig. 7(a), suggest that the degree of fractionalization is finite for the model describing the xz orbiton in $CaCu_2O_3$ and it is just a bit weaker than for the strictly 1D case of Sr_2CuO_3.

Interestingly, the degree of fractionalization is stronger in the case of the spin-orbital separation in a not-strictly 1D compound ($CaCu_2O_3$) than in the case of the spin-charge separation in completely 1D case (Sr_2CuO_3), cf. Fig. 7(a). There are three reasons for that (i) the spin excitations in the buckled spin ladder $CaCu_2O_3$ are essentially spinons on the here relevant energy scale, cf. Fig. 7(b); (ii) the motion of the orbital excitation can be 1D due to the typical directional character of orbital hoppings, cf. Fig. 7(b); (iii) the different ratio of the spinon and orbiton velocities versus spinon and holon velocities in these two cases means that the spinon can move away much quicker from the orbiton than from the holon, allowing for an 'easier' separation from the spinon in the spin-orbital case. While the first condition requires 1D spin exchange interactions and is similarly valid for the spin-charge separation phenomenon, the other two conditions are generic to the spin-orbital separation phenomenon. This means that the spin-orbital separation is in general more robust than the spin-charge separation and can be more easily observed in systems which are not strictly 1D.

VIII. Extension: Orbiton in a Quasi-2D Iridium Oxide and the Role of Jahn-Teller Effect

This part describes the content of paper [H3] (partially) and [H8]

So far we have shown that the orbiton can indeed be observed in two copper oxides: one with a purely 1D (Sr_2CuO_3, see Sec. VI) and the other one with a two-leg ladder geometry ($CaCu_2O_3$, see Sec. VII). As the latter one had a relatively small coupling between the legs of the ladders, effectively both cases were somewhat similar:

as a result of the 'mapping' between a spin-orbital problem and an effective t–J-like problem the orbiton could be seen as a hole that could easily become mobile in an antiferromagnet – due to the spin-orbital separation effect. Could the latter situation be observed in one of the quasi-2D transition metal oxides?

The theoretical discussion presented in Secs. III-IV suggested that such a situation could be quite different in higher dimensions – for instance already in 2D. Even though the mapping still holds in 2D, the orbiton should become less mobile due to the lack of spin-orbital separation in 2D and the dressing of the mobile orbiton with spin fluctuations. For example such a simple but relatively realistic 2D spin-orbital model with two inequivalent orbital hoppings was proposed in paper [H3]. Mapping that model onto the t–J model lead to effective hopping of the orbiton $t = 2t_1t_2/U$ in the effective t–J model. Here t_1 (t_2) denote the bare hopping of an electron between the nearest neighbor ground (excited) orbitals and U is the onsite Hubbard repulsion. For quasi-2D copper oxides we would typically have for the ground state $x^2 - y^2$ orbital and one of the the excited t_{2g} orbitals $t_2 \approx t_1/2$. This gives $J \approx 4t$ in the effective t–J model, since $J \approx 4t_1^2/U$. Solving such a 2D t–J model, using the well-suited to the problem mapping onto the spin polaron problem and the self-consistent Born approximation [64], would give the strongly renormalized bandwidth of the orbiton dispersion $W \approx 0.125J$, cf. Fig. 1(c)-(d) of paper [H3]. Unfortunately, this would mean that for the quasi-2D copper oxides the orbiton bandwidth W 10 meV. It therefore should not surprise us that so far the orbiton dispersion has not been detected in the quasi-2D copper oxides[9] and the *dd* excitations in these systems are typically assumed to be completely local, cf. Ref. [97].

It turns out that orbitons can be observed in a different class of quasi-2D transition metal oxides: the family of the quasi-2D '214' iridium oxides, best exemplified by Sr_2IrO_4 or Ba_2IrO_4,[10] which have a surprisingly similar crystal and electronic structure as the 'famous' quasi-2D copper oxides, see Refs. [98, 99]. Although in the ionic picture Ir^{4+} leads to a $5d^5$ configuration, the tetragonal crystal field and the relatively strong spin-orbit coupling ξ of the $5d$ iridium shell (ca. 0.4 eV, cf. [100]) hugely simplify the problem. In fact, in the hole picture the iridium ion has a single hole in the doubly degenerate ground state with an effective $j = 1/2$ total angular momentum [$j = l+s$ where $l = 1$ is the (effective) orbital angular momentum of the t_{2g} subshell and $s = 1/2$ is the spin angular momentum of a single hole]. The strong correlations localize the holes in the iridium ions leading to a Mott insulating ground state and to the low energy physics being governed by an effective interaction between $j = 1/2$ spin-orbitals. The latter follows from the superexchange processes, which are predominantly between nearest neighbor iridium ions and which, on a square lattice formed by the iridium ions in the IrO_2 planes of Sr_2IrO_4, occur to be of the Heisenberg type [101]. Consequently the ground state is magnetic, it is an antiferromagnetic order formed by the $j = 1/2$ spin-orbitals (see Fig. 8). The low energy excitations carry $j_z = 1$ quantum number and are of collective type – to show their similarity with those known for the 2D $S = 1/2$ Heisenberg antiferromagnet, they are called $j = 1/2$ magnons. The $j = 1/2$ magnon dispersion was detected by the recent RIXS experiment [102] and is well described using a linear spin wave approximation. The qualitative similarity of that low energy physics with the well-known La_2CuO_4 is striking.

The low energy excited states on the iridium ion, that lie above the manifold spanned by the states carrying the $j = 1/2$ spin-orbital quantum number (i.e. the AF ordered ground state and the magnons), resemble the orbital excitations of the cuprates. Indeed, locally i.e. on a single iridium ion, there are four states carrying $j = 3/2$ quantum number (i.e. having a different total angular momentum as the ground state) which are separated from the $j = 1/2$ states by a gap $3\xi/2$ due the spin-orbit coupling ξ. We can call these excited states '$j = 3/2$ orbitals'. Moreover, one expects that a hole in one of the $j = 3/2$ excited orbitals can swap its places with the nearest neighbor hole in the $j = 1/2$ spin-orbital via a 't^2/U' process. Consequently, due to these spin-orbital exchange processes, the $j = 3/2$ orbital excitations can acquire collective nature. While in the literature this $j = 3/2$ collective excitation is often called an 'exciton' [see Refs. [100, 102] and [H8]], it can equally well be called a '$j = 3/2$ orbiton'. Finally, as such an exchange process happens in an antiferromagnet, the $j = 3/2$ orbiton has to strongly couple to the $j = 1/2$ magnons, just as could be expected from the 'mapping' between such a spin-orbital problem and an effective t–J problem, cf. Fig. 8(a).

This interesting but pretty complex physics of the quasi-2D iridates would probably not be worth studying, if not for the fact that it can be very nicely seen in the RIXS experiment. Indeed, the RIXS spectrum taken on the iridium L_3 edge of Sr_2IrO_4 [100, 102], reveals a rather complicated spectrum of the $j = 3/2$ orbital excitations, cf. Fig. 3 of Ref. [100] but with a clear onset of the strong dispersion and a large incoherent continuum. Nevertheless, the spectrum is quite well-described by the spin-orbital model which contains the spin-orbital exchange processes and the mapping onto an effective t–J like problem, as described above [100, 102]. The only discrepancy lies in the unexplained feature with the minimum at the Γ point that was observed in the normal incidence RIXS spectrum, cf. Fig. 3(a) and 4(b) in Ref. [100]. It was the main task of paper [H8] to explain this feature. Thus, below we

[9] A small dispersion of the orbital excitations was detected in the *doped* quasi-2D copper oxides [96]. However, due to doping, that dispersion might be closely related to the motion of doped holes in these compounds.

[10] Often jointly called as the '2-1-4 iridates' (which differentiates them from the '2-1-3 iridates' with the honeycomb lattices).

briefly show how to derive and solve the model which includes the propagation of the $j = 3/2$ orbiton due to the Jahn-Teller effect:

- Our starting point here is the Jahn-Teller effect for the t_{2_g} electrons. In this case, as a result of the electron-phonon interaction, the orbital operators $\mathbf{l}$ couple to the tetragonal phonon modes Q_2 and Q_3 (the e_g modes) and to the trigonal phonon modes Q_4, Q_5, and Q_6 (the t_{2g} modes). After integrating out the phonons, the Jahn-Teller interaction is expressed solely in terms of the (effective) orbital angular momentum operator $\mathbf{l}$ [12]:

$$\mathcal{H}_{\rm JT} = V\sum_{\langle \mathbf{i},\mathbf{j}\rangle}\left[\left(l^z_{\mathbf{i}}\right)^2-\frac{2}{3}\right]\left[\left(l^z_{\mathbf{j}}\right)^2-\frac{2}{3}\right]+V\sum_{\langle \mathbf{i},\mathbf{j}\rangle}\left[\left(l^x_{\mathbf{i}}\right)^2-\left(l^y_{\mathbf{i}}\right)^2\right]\left[\left(l^x_{\mathbf{j}}\right)^2-\left(l^y_{\mathbf{j}}\right)^2\right]+\kappa V\sum_{\langle \mathbf{i},\mathbf{j}\rangle}\Big[\left(l^x_{\mathbf{i}}l^y_{\mathbf{i}}+l^y_{\mathbf{i}}l^x_{\mathbf{i}}\right)\times \left(l^x_{\mathbf{j}}l^y_{\mathbf{j}}+l^y_{\mathbf{j}}l^x_{\mathbf{j}}\right)+...\Big] \tag{16}$$

  where V (κV) is the strength of the Jahn-Teller interaction due to the coupling to the t_{2g} (e_g) phonons. Since the Jahn-Teller coupling constant for t_{2g} phonons is typically much smaller one can safely set $\kappa = 0.1$. On the other hand, the precise value of the Jahn-Teller interaction is at present unclear and is left here as a free parameter.

- Due to the strong spin-orbit coupling, it is convenient to express the Jahn-Teller interaction $\mathcal{H}_{\rm JT}$ in the eigenbasis of the total angular momentum operator $\mathbf{j} = \mathbf{l} + \mathbf{s}$, see paper [H8]. The terms of the resulting Hamiltonian can be grouped into three classes

$$\mathcal{H}_{\rm JT} = \mathcal{H}_{\rm JT}(1/2,1/2)+\mathcal{H}_{\rm JT}(3/2,1/2)+\mathcal{H}_{\rm JT}(3/2,3/2), \tag{17}$$

  where the first terms $\mathcal{H}_{\rm JT}(1/2,1/2)$ denote the Jahn-Teller interaction between two $j = 1/2$ total angular momenta, the terms $\mathcal{H}_{\rm JT}(3/2,1/2)$ describe the interaction between one $j = 1/2$ and one $j = 3/2$ total angular momentum, and the last terms $\mathcal{H}_{\rm JT}(3/2,3/2)$ express the interactions between two $j = 3/2$ total angular momenta. Interestingly, the first terms vanish here, reflecting the well-known [12] quenching of orbital physics within the $j = 1/2$ subshell. At the same time the last term $\mathcal{H}_{\rm JT}(3/2,3/2)$ only contributes if a large number of $j = 3/2$ states are present and is strongly suppressed at large ξ. Consequently, these are the middle terms, $\mathcal{H}_{\rm JT}(3/2,1/2)$, that become relevant when RIXS raises a single hole from the $j = 1/2$ into a $j = 3/2$ state [100, 102].

- Ultimately, as in the other section, we intend to calculate the spectral function for a single $j = 3/2$ orbiton ($|\chi_{\mathbf{k},j_z}\rangle$, where $j_z = \pm 3/2, \pm 1/2$) added to the AF $j = 1/2$ ground state ($|0\rangle$) and with the dynamics given by the Jahn-Teller Hamiltonian $\mathcal{H}_{\rm JT}(3/2,1/2)$ as well as the superexchange Hamiltonian known from Refs. [100, 102] ($\mathcal{H}_{\rm SE}$),

$$O(\mathbf{k},\omega) = \frac{1}{\pi}\lim_{\eta\to 0}\Im{\rm Tr}_{j_z}\Big\langle 0\Big|\chi_{\mathbf{k},j_z}\frac{1}{\omega-\mathcal{H}_{\rm JT}(3/2,1/2)-\mathcal{H}_{\rm SE}+i\delta}\chi^\dagger_{\mathbf{k},j_z}\Big|0\Big\rangle. \tag{18}$$

- To this end, we map the above problem of the orbiton propagation directly onto an effective spin polaron problem [64]. We note that, although this mapping is inspired and is closely related to the mapping onto the t–J model presented in Sec. III, it is also quite distinct: (i) on one hand, it is only valid in the presence of long range order; (ii) on the other hand, it can allow for the change of the j_z quantum number of the orbiton. As a result the Jahn-Teller Hamiltonian reads

$$\mathcal{H}_{\rm JT}(3/2,1/2) = \sum_{\mathbf{k}}\hat{E}^{\rm JT}_{\mathbf{k}}\hat{\chi}^\dagger_{\mathbf{k}}\hat{\chi}_{\mathbf{k}}+\sum_{\mathbf{k},\mathbf{q}}\left(\hat{M}^{\rm JT}_{\mathbf{k},\mathbf{q}}\hat{\chi}^\dagger_{\mathbf{k}}\hat{\chi}_{\mathbf{k}-\mathbf{q}}a_{\mathbf{q}}+h.c.\right), \tag{19}$$

  where $\hat{\chi}^\dagger_{\mathbf{k}}$ is a vector of four creation operators that create a $j = 3/2$ orbiton with one of the four j_z quantum numbers and $a_{\mathbf{q}}$ creates a magnon with momentum $\mathbf{q}$. The detailed expressions for the free hopping of the $j = 3/2$ orbitons ($\hat{E}^{\rm JT}_{\mathbf{k}}$) as well as the interactions of the $j = 3/2$ orbitons with magnons ($\hat{M}^{\rm JT}_{\mathbf{k},\mathbf{q}}$) are given in [H8]. There, also the detailed expression for $\mathcal{H}_{\rm SE}$ is given.

- Finally, the orbital spectral function Eq. (18), is calculated using, the well-suited to the polaronic problems, self-consistent Born approximation [64].

The orbiton spectral function calculated using not only the superexchange but also the Jahn-Teller model reproduces well the experimental RIXS spectrum of Refs. [100, 102], see Fig. 2 of [H8]. In particular, due to the Jahn-Teller interaction an additional feature with the minimum at the Γ point occurs in the spectrum and therefore the experimental RIXS spectrum is fully explained.

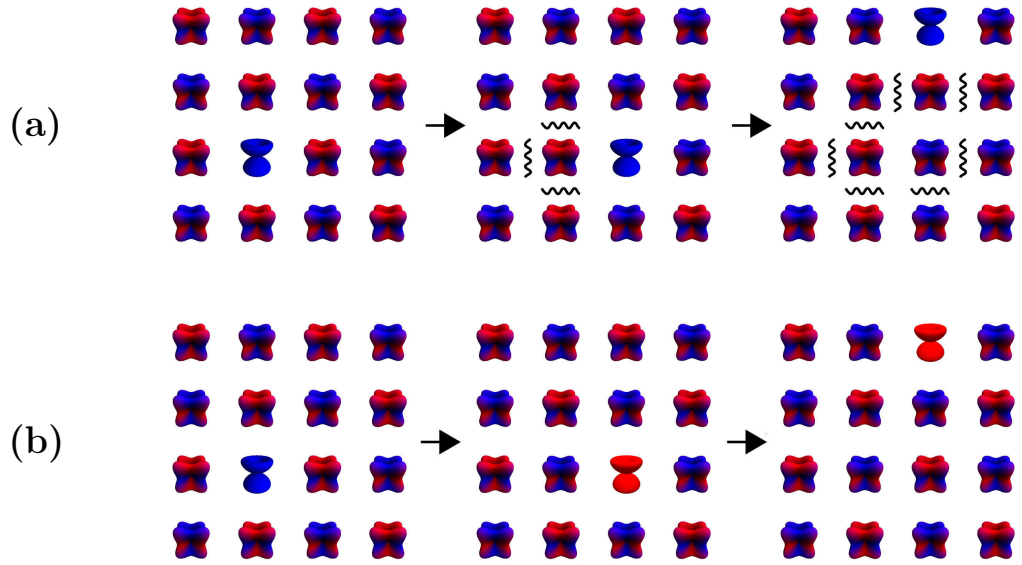

Figure 8: **Propagation of a $j = 3/2$ orbiton in the $j = 1/2$ antiferromagnetic order of Sr_2IrO_4** (a) Cartoon showing such a propagation via the polaronic hopping (due to Jahn-Teller effect *or* superexchange): a $j = 3/2$ orbiton with the $j_z = -3/2$ quantum number (left panel) does not change its j_z quantum number during the hopping process to the nearest neighbor sites (middle / right panels) and thus the $j = 1/2$ magnons are created at each step of the hopping of an orbiton (wiggle lines on middle and right panels). (b) Cartoon showing such a propagation via the free hopping (solely due to Jahn-Teller effect): a $j = 3/2$ orbiton with the $j_z = -3/2$ quantum number (left panel) hops to the nearest neighbor site and acquires $j_z = 3/2$ quantum number (middle panel). Note that in this case the $j = 1/2$ magnons are *not* created in the system (middle / right panels). [Panels and caption adopted from Fig. 4 of paper [H8]]

It is interesting to understand whether the Jahn-Teller effect can lead to a qualitatively distinct propagation of the $j = 3/2$ orbiton than the superexchange mechanism. It turns out that the difference between these two mechanisms for orbiton propagation in the quasi-2D iridate is of fundamental nature. The crucial aspect concerns the nearest-neighbor processes, which are depicted for superexchange and Jahn-Teller effect in Fig. 8. In superexchange, the $j = 3/2$ orbiton propagates by exchanging place with an $j = 1/2$ spin-orbital while both conserve their j_z quantum number. In the ground state given by the $j = 1/2$ antiferromagnetic order, where nearest neighbors are always of opposite j_z, this necessarily creates or removes 'defects', see Fig. 8(a), i.e. the $j = 1/2$ magnons. On the other hand, the Jahn-Teller effect allows the $j = 3/2$ orbiton and the $j = 1/2$ spin-orbital to flip their j_z quantum numbers while exchanging places and this allows for the nearest neighbor hopping of a $j = 3/2$ orbiton without creating $j = 1/2$ magnons, i.e. a free orbiton dispersion, see Fig. 8(b). The origin of the difference lies in the fact that the electronic hopping driving the superexchange conserves the j_z quantum number, while the lattice-mediated Jahn-Teller effect is insensitive to the orbital phase. This allows j_z to change during the Jahn-Teller–driven propagation.

IX. Conclusions and New Perspectives for the Orbital Physics

This review discusses the problem of the propagation of collective orbital excitation (orbiton) in several distinct strongly correlated systems that, however, all bear an antiferromagnetic ground state. From the theoretical point of view, *the most interesting result concerns the mapping of the problem of an orbiton propagation in such an antiferromagnetic ground state onto a problem of a single hole in an effective half-filed t–J model* [H1]. That result has inspired few theoretical works on the problem of the so-called spin-orbital separation [103–105] (as well as [H6-H7]) and has greatly helped in understanding several experimental results on the orbiton dispersion found by the resonant inelastic x-ray scattering (RIXS) experiments. The models describing these experiments on an almost quantitative level were discussed in detail in this review: in the quasi-1D cuprate [H2, H4], in the ladder-like cuprate [H5], and in the quasi-2D iridates [100, 102] (as well as [H8]). The latter studies have also allowed us to learn more about the various aspects related to the orbiton propagation – such as e.g.: the importance of various superexchange processes for the realistic description of the orbiton motion [H2, H4], the robustness of the spin-orbital separation [H5], or the role that could be played by the Jahn-Teller effect in the propagation of orbitons [H8].

What seem to be the most challenging problems in the coming years? Probably the most apparent problem, which directly follows from the studies presented in this review, concerns the *observation of the orbiton propagation in*

the quasi-2D cuprates. As already mentioned, so far all of the orbital excitations observed in the RIXS experiments one thse compounds seemed to have a purely local character. There is a general belief, that is also supported by simple calculations [H3], that this is solely due to the too small resolution of the current RIXS experiments. However, the newly installed RIXS ID-32 beamline in European Synchrotron Radiation Facility (ESRF), that had already been exploited to beautifully uncover the dispersion of magnons in several cuprates [9], should be capable in measuring the orbiton dispersion with a far better resolution. Indeed, private communication with several RIXS groups suggests that in the near future several RIXS experiments dedicated to this problem are planned. We are awaiting for these results with a great interest.

Another open question is more theoretical – it concerns a far *better understanding the role played by the electron-phonon coupling in the orbiton propagation*. For instance, having seen how important the Jahn-Teller effect is for the orbiton propagation in the quasi-2D iridates, one can wonder why the electron-phonon interaction was *not* included in the reported above studies of the orbiton propagation in the quasi-1D or ladder-like cuprates. Moreover, although that was not discussed in the Introduction, it is well-known that the Jahn-Teller effect is extremely important for the understanding of the onset of orbitally ordered phases in several 'classical' orbital systems, such as $KCuF_3$ or $LaMnO_3$ [12, 15].

While a definite answer to this problem is not clear, one can speculate as follows: The Jahn-Teller effect turned out to be important for the quasi-2D iridates, since it allowed a channel of the 'free' orbiton propagation between nearest neighbor sites. Note that, without Jahn-Teller and restricting solely to nearest neighbor processes, the orbiton is strongly coupled to magnons and in 2D can only move by dressing with magnons. At the same time, in the case of the lower-dimensional cuprates, the orbiton is in any case relatively 'free' – which is due to the spin-orbital separation. Therefore, any extra channel that allows for 'free' propagation is not that relevant. Nevertheless, a thorough study on the role of the electron-phonon coupling on the orbiton propagation is needed. Such a study should not only be contrasted with the findings presented in this review but also with the earlier studies [106–108] that suggested that the electron-phonon played an important (and destructive) role in the orbiton propagation [106–108].

References

[1] P. W. Anderson, Science **177**, 393 (1972).

[2] D. I. Khomskii, *Basic Aspects of the Quantum Theory of Solids: Order and Elementary Excitations* (Cambridge University Press, Cambridge, 2010).

[3] M. Imada, A. Fujimori, and Y. Tokura, Rev. Mod. Phys. **70**, 1039 (1998).

[4] A. Auerbach, *Interacting Electrons and Quantum Magnetism* (Springer, New York, 1994).

[5] P. A. Lee, N. Nagaosa, and X.-G. Wen, Rev. Mod. Phys. **78**, 17 (2006).

[6] J. Zaanen, G. A. Sawatzky, and J. W. Allen, Phys. Rev. Lett. **55**, 418 (1985).

[7] R. Coldea *et al.*, Phys. Rev. Lett. **86**, 5377 (2001).

[8] L. Braicovich *et al.*, Phys. Rev. Lett. **102**, 167401 (2009).

[9] Y. Y. Peng *et al.*, Nature Physics **13**, 1201 (2017).

[10] J. Zaanen, Nature Physics **9**, 609 (2013).

[11] J. S. Griffith, *The Theory of Transition Metal Ions* (Cambridge University Press, Cambridge, 1964).

[12] K. I. Kugel and D. I. Khomskii, Sov. Phys. Usp. **25**, 231 (1982).

[13] Y. Tokura and N. Nagaosa, Science **288**, 462 (2000).

[14] A. M. Oleś, L. Felix Feiner, and J. Zaanen, Phys. Rev. B **61**, 6257 (2000).

[15] A. M. Oleś, G. Khaliullin, P. Horsch, and L. F. Feiner, Phys. Rev. B **72**, 214431 (2005).

[16] W. Brzezicki and A. M. Oleś, Phys. Rev. B **83**, 214408 (2011).

[17] W. Brzezicki, J. Dziarmaga, and A. M. Oleś, Phys. Rev. B **87**, 064407 (2013).

[18] P. Czarnik, J. Dziarmaga, and A. M. Oleś, Phys. Rev. B **96**, 014420 (2017).

[19] L. F. Feiner, A. M. Oleś, and J. Zaanen, Phys. Rev. Lett. **78**, 2799 (1997).

[20] S. Kadota, I. Yamada, S. Yoneyama, and K. Hirakawa, Journal of the Physical Society of Japan **23**, 751 (1967).

[21] E. Pavarini, E. Koch, and A. I. Lichtenstein, Phys. Rev. Lett. **101**, 266405 (2008).

[22] J. C. T. Lee *et al.*, Nature Physics **8**, 63 (2011).
[23] W.-L. You, G.-S. Tian, and H.-Q. Lin, Phys. Rev. B **75**, 195118 (2007).
[24] E. Saitoh *et al.*, Nature **410**, 180 (2001).
[25] B. Lake, D. A. Tennant, and S. E. Nagler, Phys. Rev. Lett. **85**, 832 (2000).
[26] K. I. Kugel and D. I. Khomskii, JETP **37**, 725 (1973).
[27] H. F. Pen, J. van den Brink, D. I. Khomskii, and G. A. Sawatzky, Phys. Rev. Lett. **78**, 1323 (1997).
[28] S. Ishihara and S. Maekawa, Phys. Rev. B **62**, 2338 (2000).
[29] F. Forte, L. J. P. Ament, and J. van den Brink, Phys. Rev. Lett. **101**, 106406 (2008).
[30] P. Marra, K. Wohlfeld, and J. van den Brink, Phys. Rev. Lett. **109**, 117401 (2012).
[31] S. Ishihara, Phys. Rev. B **69**, 075118 (2004).
[32] S.-I. Shamoto *et al.*, Journal of Neutron Research **13**, 175 (2005).
[33] M. Grüninger *et al.*, Nature **418**, 39 (2002).
[34] L. J. P. Ament *et al.*, Review of Modern Physics **83**, 705 (2011).
[35] R. M. Macfarlane and J. W. Allen, Phys. Rev. B **4**, 3054 (1971).
[36] D. Polli *et al.*, Nature Mater. **6**, 643 (2007).
[37] C. Ulrich *et al.*, Phys. Rev. Lett. **103**, 107205 (2009).
[38] J. Kanamori, Journal of Physics and Chemistry of Solids **10**, 87 (1959).
[39] J. B. Goodenough, *Magnetism and the Chemical Bond* (Interscience, New York, 1963).
[40] F. Mila, European Journal of Physics **21**, 499 (2000).
[41] A. M. Oleś, P. Horsch, L. F. Feiner, and G. Khaliullin, Phys. Rev. Lett. **96**, 147205 (2006).
[42] G. Khaliullin and V. Oudovenko, Phys. Rev. B **56**, R14243 (1997).
[43] G. Khaliullin and S. Maekawa, Phys. Rev. Lett. **85**, 3950 (2000).
[44] K. Kikoin, O. Entin-Wohlman, V. Fleurov, and A. Aharony, Phys. Rev. B **67**, 214418 (2003).
[45] K. Wohlfeld, A. M. Oleś, and P. Horsch, Phys. Rev. B **79**, 224433 (2009).
[46] A. Herzog, P. Horsch, A. M. Oleś, and J. Sirker, Phys. Rev. B **83**, 245130 (2011).
[47] W.-L. You, A. M. Oleś, and P. Horsch, Phys. Rev. B **86**, 094412 (2012).
[48] Y.-Q. Li, M. Ma, D.-N. Shi, and F.-C. Zhang, Phys. Rev. B **60**, 12781 (1999).
[49] M. Karbach and G. Müller, Phys. Rev. B **62**, 14871 (2000).
[50] M. Karbach, D. Biegel, and G. Müller, Phys. Rev. B **66**, 054405 (2002).
[51] P. Jordan and E. Wigner, Z. Physik **47**, 631 (1928).
[52] K. A. Chao, J. Spałek, and A. M. Oleś, J. Phys. C **10**, L271 (1977).
[53] J. Spałek, Acta Physica Polonica A **111**, 409 (2007).
[54] S. Barnes and S. Maekawa, Journal of Physics: Condensed Matter **14**, L19 (2002).
[55] C. Kim *et al.*, Phys. Rev. Lett. **77**, 4054 (1996).
[56] H. Suzuura and N. Nagaosa, Phys Rev B **56**, 3548 (1997).
[57] M. Brunner, F. Assaad, and A. Muramatsu, Eur. Phys. J. B **16**, 209 (2000).
[58] B. J. Kim *et al.*, Nature Physics **2**, 397 (2006).
[59] A. Moreno, A. Muramatsu, and J. M. P. Carmelo, Phys. Rev. B **87**, 075101 (2013).
[60] E. H. Lieb and F. Y. Wu, Phys. Rev. Lett. **20**, 1445 (1968).
[61] A. Luther and V. J. Emery, Phys. Rev. Lett. **33**, 589 (1974).
[62] W. F. Brinkman and T. M. Rice, Phys. Rev. B **2**, 1324 (1970).
[63] S. Schmitt-Rink, C. M. Varma, and A. E. Ruckenstein, Phys. Rev. Lett. **60**, 2793 (1988).
[64] G. Martinez and P. Horsch, Phys. Rev. B **44**, 317 (1991).
[65] Y. F. Kung *et al.*, Phys. Rev. B **96**, 195106 (2017).
[66] B. Sutherland, Phys. Rev. B **12**, 3795 (1975).

[67] Y. Q. Li, M. Ma, D. N. Shi, and F. C. Zhang, Phys. Rev. Lett. **81**, 3527 (1998).
[68] Y. Yamashita, N. Shibata, and K. Ueda, Phys. Rev. B **61**, 4012 (2000).
[69] W. Yu and S. Haas, Phys. Rev. B **63**, 024423 (2000).
[70] G. Baskaran, Z. Zou, and P. Anderson, Solid State Communications **63**, 973 (1987).
[71] I. Affleck and J. B. Marston, Phys. Rev. B **37**, 3774 (1988).
[72] D. P. Arovas and A. Auerbach, Phys. Rev. B **38**, 316 (1988).
[73] M. M. Maśka, Phys. Rev. B **57**, 8755 (1998).
[74] D. Sénéchal, D. Perez, and M. Pioro-Ladrière, Phys. Rev. Lett. **84**, 522 (2000).
[75] F. Moussa *et al.*, Phys. Rev. B **54**, 15149 (1996).
[76] Y.-Q. Li, M. Ma, D.-N. Shi, and F.-C. Zhang, Phys. Rev. B **60**, 12781 (1999).
[77] A. Klauser, J. Mossel, J.-S. Caux, and J. van den Brink, Phys. Rev. Lett. **106**, 157205 (2011).
[78] M. Raczkowski and F. F. Assaad, Phys. Rev. B **88**, 085120 (2013).
[79] W.-L. You, A. M. Oleś, and P. Horsch, Phys. Rev. B **86**, 094412 (2012).
[80] Y. Chen, Z. D. Wang, Y. Q. Li, and F. C. Zhang, Phys. Rev. B **75**, 195113 (2007).
[81] R. Lundgren, V. Chua, and G. A. Fiete, Phys. Rev. B **86**, 224422 (2012).
[82] T. Ami *et al.*, Phys. Rev. B **51**, 5994 (1995).
[83] N. Motoyama, H. Eisaki, and S. Uchida, Phys. Rev. Lett. **76**, 3212 (1996).
[84] K. M. Kojima *et al.*, Phys. Rev. Lett. **78**, 1787 (1997).
[85] H. Fujisawa *et al.*, Phys. Rev. B **59**, 7358 (1999).
[86] M. van Veenendaal, Phys. Rev. Lett. **96**, 117404 (2006).
[87] J. C. Slater and G. F. Koster, Phys. Rev. **94**, 1498 (1954).
[88] R. Neudert *et al.*, Phys. Rev. B **62**, 10752 (2000).
[89] J. B. Grant and A. K. McMahan, Phys. Rev. B **46**, 8440 (1992).
[90] J. Zaanen and A. M. Oleś, Phys. Rev. B **37**, 9423 (1988).
[91] A. C. Walters *et al.*, Nature Physics **5**, 867 (2009).
[92] B. Lake *et al.*, Nature Physics **6**, 50 (2010).
[93] E. Bordas, C. de Graaf, R. Caballol, and C. J. Calzado, Phys. Rev. B **71**, 045108 (2005).
[94] H.-Y. Huang *et al.*, Physical Review B **84**, 235125 (2011).
[95] K. Koepernik and H. Eschrig, Phys. Rev. B **59**, 1743 (1999).
[96] D. S. Ellis *et al.*, Phys. Rev. B **92**, 104507 (2015).
[97] M. Moretti Sala *et al.*, New Journal of Physics **13**, 043026 (2011).
[98] B. J. Kim *et al.*, Phys. Rev. Lett. **101**, 076402 (2008).
[99] F. Wang and T. Senthil, Phys. Rev. Lett. **106**, 136402 (2011).
[100] J. Kim *et al.*, Nature Communications **5**, 4453 (2014).
[101] G. Jackeli and G. Khaliullin, Phys. Rev. Lett. **102**, 017205 (2009).
[102] J. Kim *et al.*, Phys. Rev. Lett. **108**, 177003 (2012).
[103] B. Kumar, Phys. Rev. B **87**, 195105 (2013).
[104] W. Brzezicki, J. Dziarmaga, and A. M. Oleś, Phys. Rev. Lett. **112**, 117204 (2014).
[105] D. Vieira, Journal of Chemical Theory and Computation **10**, 3641 (2014).
[106] P. B. Allen and V. Perebeinos, Phys. Rev. Lett. **83**, 4828 (1999).
[107] J. van den Brink, Phys. Rev. Lett. **87**, 217202 (2001).
[108] K. P. Schmidt, M. Grüninger, and G. S. Uhrig, Phys. Rev. B **76**, 075108 (2007).

5 Discussion of other scientific (artistic) achievements.

Except for points (a) and (b) below, so far my research on strongly correlated electron systems can be grouped into two classes of problems: (i) understanding the collective excitations in these systems and their appearance in the resonant inelastic x-ray scattering experiments [papers [H1-H8] in part 4(c) as well as points (d-f) and (h) below], (ii) understanding the single particle excitations in these systems and their appearance in photoemission experiments [points (c) and (g) below]. These two classes of problems are of course closely related to each other: for instance due to the mentioned in part 4(c) 'mapping' of the orbiton problem onto an effective t–J model problem or due to the importance of the same physical mechanisms (such as for example the mentioned below 'three-site terms').

(a) Coexistence of Metallic and Magnetic Phase in Doped Vanadates [master thesis]:

[a1] **K. Wohlfeld**, A. M. Oleś, **2006**, "Double exchange model in cubic vanadates", **Physica Status Solidi (b)**, 243, 142.

[a2] **K. Wohlfeld**, **2006**, "Double exchange model for correlated electrons in systems with t_{2g} orbital degeneracy", **AIP Conf. Proc.**, 846, 295.

The doped cubic vanadates, best exemplified by $La_{1-x}Sr_xVO_3$, are relatively rare systems, for they show a coexistence of a metallic and C-type antiferromagnetic (C-AF) phase for $x \sim 0.2$ strontium doping. To explain this phase, in papers [a1-a2] we formulate a 'double exchange model via t_{2g} degenerate orbitals'. The model treats the localized electrons in the $3d_{xy}$ orbitals as classical $S = 1/2$ spins, which interact by Hund's exchange J_H with the partly filled and degenerate $3d_{yz}$ and $3d_{xz}$ electrons. Using the slave-boson mean-field method we demonstrate in [a1] that, due to the relative weakness of this double exchange mechanism, the anisotropic C-AF *and* metallic phase can be stabilized. It occurs that a simple Hartree-Fock approximation is not enough to obtain the correct solution of this double exchange model [a2]. This means that the constraint of the double occupancies, that is inherently present in this model, has to be treated at least on the slave-boson mean-field level.

Interestingly, the above results stays in contrast with the far better known problem of doped manganites. In that case the double exchange mechanism via the e_g degenerate orbitals can stabilize a uniform ferromagnetic order in the hole-doped regime of the manganites. Such distinct properties of these two models stem from the different symmetries of the hopping elements within the t_{2g} and the e_g subshell.

(b) Charge Density Wave in $Sr_{14-x}Ca_xCu_{24}O_{41}$ [part of the PhD thesis (partially finished after the PhD defence)]:

[b1] **K. Wohlfeld**, A. M. Oleś, G. A. Sawatzky, **2007**, "Origin of charge density wave in the coupled spin ladders of $Sr_{14-x}Ca_xCu_{24}O_{41}$", **Physical Review B**, 75, 180501(R).

[b2] **K. Wohlfeld**, A. M. Oleś, G. A. Sawatzky, **2007**, "Charge density wave in the spin ladder of $Sr_{14-x}Ca_xCu_{24}O_{41}$", **Physica C**, 460, 1043.

[b3] **K. Wohlfeld**, **2007**, "Doped Spin Ladder: Zhang-Rice Singlets or Rung-centred Holes?", **AIP Conf. Proc.**, 918, 337.

[b4] **K. Wohlfeld**, A. M. Oleś, G. A. Sawatzky, **2010**, "Charge density wave in Sr_{14-x} $Ca_xCu_{24}O_{41}$", **Physica Status Solidi (b)**, 247, 668.

[b5] **K. Wohlfeld**, A. M. Oleś, G. A. Sawatzky, **2010**, "t–J model of coupled Cu_2O_5 ladders in $Sr_{14-x}Ca_xCu_{24}O_{41}$", **Physical Review B**, 81, 214522.

In the above papers we try to understand the origin of a charge density wave (CDW) in Sr_{14-x} $Ca_xCu_{24}O_{41}$. It turns out that in these ladder–like cuprate systems, a CDW with period 3 as well as with period 5 could experimentally be observed (the precise periodicity depends on the doping level). However, a CDW with period 4 was not observed in these copper oxides. That is a rather striking result, since the simple t–J calculations for a single ladder would solely predict a CDW with period 2 or 4 – but not 3 or 5.

In papers [b1-b3] we discuss a charge transfer model for the Cu_2O_5 spin ladders. In paper [b1] first a single ladder is taken into account. The model is solved using Hartee-Fock approximation and the CDW with the odd *and* even period can become stable for realistic parameters of the model. However, the inclusion of the interladder interactions favors (disfavors) the stability of the CDW with odd (even) periodicity, respectively. Papers [b2-b3] discuss in more detail the problem of the local distribution of the doped holes forming the 'additional charge' in the CDW state: a profound stability of the of the Zhang-Rice singlets with respect to other configurations of doped holes (such a the rung-centred holes) is found. All of these results stay in agreement with the x-ray absorption experiments performed on Sr_{14-x} $Ca_xCu_{24}O_{41}$.

Having seen that the charge transfer for coupled ladders can explain the onset of the CDW with an odd period in Sr_{14-x} $Ca_xCu_{24}O_{41}$, one can wonder whether an extension of the standard t–J model on a ladder can support this ordered state. Such a study was performed in [b5] (with a preliminary result, which concerns two coupled chains, shown in paper [b4]) and the answer is positive: A detailed derivation shows that the ladder t–J model has to be supplemented by the Coulomb repulsion (V) between holes in the neighboring ladders. Indeed, a mean-field solution of the derived t–J–V model may explain the onset of the charge density wave with the odd period.

(c) Properties of Orbital and Spin-Orbital Polarons [part of the PhD thesis]:

[c1] M. Daghofer, **K. Wohlfeld**, A. M. Oleś, E. Arrigoni, P. Horsch, **2008**, "Absence of hole confinement in transition metal oxides with orbital degeneracy", **Physical Review Letters**, 100, 066403.

[c2] **K. Wohlfeld**, M. Daghofer, A. M. Oleś, P. Horsch, **2008**, "Spectral properties of orbital polarons in Mott insulators", **Physical Review B**, 78, 214423.

[c3] **K. Wohlfeld**, **2008**, "Polaron in the t-J models with three-site terms: the $SU(2)$ and the Ising cases", **AIP Conf. Proc.**, 1014, 265.

[c4] **K. Wohlfeld**, A. M. Oleś, M. Daghofer, P. Horsch, **2009**, "Reiter's wavefunction applied to a t_{2g} orbital t–J model", **Acta Physica Polonica A**, 115, 110.

[c5] **K. Wohlfeld**, A. M. Oleś, P. Horsch, **2009**, "Orbitally induced string formation in the spin-orbital polarons", **Physical Review B**, 79, 224433.

[c6] **K. Wohlfeld**, **2009**, "Spin, orbital, and spin-orbital polarons in transition metal oxides", **AIP Conf. Proc.**, 1162, 220.

Understanding what happens to a strongly correlated system when, using hole or electron *doping*, it is driven away from the Mott-insulating limit with a commensurate number of electrons per ion is probably one of the most interesting problems of the correlated electron systems. In particular, understanding a filling-controlled metal – (Mott-)insulator transition is a prerequisite in unravelling the still unresolved nature of the high-temperature superconductivity of the cuprates.

It is generally assumed, that the simplest possible case of the doped Mott insulator can be realized in a commensurate Mott insulator doped with a *single* hole (or electron). Experimentally, such a case corresponds to photoemission or inverse photoemission spectra of the undoped Mott insulators (called ARPES if measured with an angular resolution). This rather peculiar limit can be solved relatively easily and, for the case of the quasi-2D cuprates or t–J-like models, it results in the added hole forming a slowly mobile spin polaron. In fact, that case was discussed in Sec. IV of 4(c) as it corresponds to the problem that arises following the mapping of the 2D spin-orbital problem.

In papers [c1-c6] we wanted to understand how such a spin polaron problem is modified when: (i) the spin degrees of freedom are integrated out but the correlated orbital degrees of freedom matter [c1-c4], and (ii) when both spin and orbital degrees of freedom are important. As for the first problem [c1-c3], we showed that a single hole added to a 2D strongly correlated system with localised t_{2g} orbital degrees of freedom is almost confined and the small residual motion of the hole can only follow if the usually neglected three-site terms are taken into account (such terms should in principle be present in any low energy t–J-like model but are usually neglected). While in paper [c1] we introduced this problem and sketched the general solution using the self-consistent Born approximation and variational cluster approximation, in the follow-up papers [c2-c4] we studied in far more detail this problem, by *inter alia* comparing its solution to those known for other (simpler) models [c2-c3] or by looking at the wavefunction of the single hole [c4].

A bit different problem was discussed in [c5-c6] – here, on top of the t_{2g} orbital degrees of freedom, also the spin degrees of freedom are taken into account. A somewhat counterintuitive result, obtained using the self-consistent Born approximation, shows that the hole is again almost confined in such a system. This means that, on a qualitative level, adding the spin degrees of freedom do not change the low energy physics of the problem.

(d) Theory of Resonant Inelastic X-ray Scattering (RIXS) [research after PhD]:

[d1] P. Marra, **K. Wohlfeld**, J. van den Brink, **2012**, "Unravelling orbital correlations with magnetic resonant inelastic x-ray scattering", **Physical Review Letters**, 109, 117401.

[d2] P. Marra, S. Sykora, **K. Wohlfeld**, J. van den Brink, **2013**, "Resonant Inelastic X-Ray Scattering as a Probe of the Phase and Excitations of the Order Parameter of Superconductors", **Physical Review Letters**, 110, 117005.

[d3] T. P. Devereaux, A. M. Shvaika, K. Wu, **K. Wohlfeld**, C. J. Jia, Y. Wang, B. Moritz, L. Chaix, W.-S. Lee, Z.-X. Shen, G. Ghiringhelli, L. Braicovich, **2016**, "Directly characterizing the relative strength and momentum dependence of electron-phonon coupling using resonant inelastic x-ray scattering", **Physical Review X**, 6, 041019.

[d4] C. J. Jia*, **K. Wohlfeld***, Y. Wang, B. Moritz, T. P. Devereaux, **2016**, "Using RIXS to uncover elementary charge and spin excitations in correlated materials", **Physical Review X**, 6, 021020. [*Authors contributed equally]

As a result of the huge improvements in the resolution of the Resonant Inelastic X-ray Scattering (RIXS) beamlines at various synchotrons around the world, the last decade has seen a 'renaissance' of the RIXS experiments. The RIXS technique has an advantage of being an atomic-specific and momentum-resolved probe of the low energy excitations. Therefore, in principle it is a perfect probe of the collective excitations that are ubiquitously found in various transition metal oxides. Unfortunately, understanding what is the sensitivity of RIXS to particular collective excitations in a given crystal is rather complex. This is because RIXS is a resonant probe and to a genuine calculation of the RIXS cross section take into account the dynamics of the so-called intermediate state of RIXS. It is only then that a connection between RIXS and various two-particle Green's functions could be established.

The first three papers mentioned above [d1-d3] discuss the following problem: Given an approximate but generally accepted treatment of the RIXS intermediate states, which in the literature is termed as fast collision approximation, their aim is to study what RIXS measures in particular condensed matter systems. Paper [d1] presents the RIXS spectra for systems with the orbital and magnetic order. It turns out that, unlike in the inelastic neutron scattering, the RIXS magnetic spectra with alternating orbital order have an extra magnon branch compared to the ferroorbital order. Paper [d2] shows that as a result of RIXS being sensitive to the charge dynamical structure factor, the superconducting gap should be visible in the RIXS spectra. Finally, even though RIXS is in principle directly sensitive only to electronic excitations, it could also indirectly measure the phonon excitations thanks to the ubiquitous electron-phonon coupling [d3]. In fact, paper [d3] suggests that RIXS can be regarded as one of the best momentum-resolved probes of the electron-phonon coupling.

The main assumption of papers [d1-d3] is that the RIXS cross section can be calculated using the fast collision approximation. In the case of the single band Hubbard–like systems this means that, depending on the polarization of the incoming and outgoing photons, RIXS is sensitive to the spin or charge dynamical structure factor. In paper [d4] we question this assumption and show that indeed the spectra calculated using this assumption have rather different spectral weights than those calculated using the exact expression for RIXS. Fortunately, the excited states probed by RIXS on single-band Hubbard models are the same as those probed by the spin and charge dynamical structure factor.

(e) Theoretical Support for Resonant Inelastic X-ray Scattering (RIXS) Experiments [research after PhD]:

[e1] E. Benckiser, L. Fels, G. Ghiringhelli, M. Moretti Sala, T. Schmitt, J. Schlappa, V. N. Strocov, N. Mufti, G. R. Blake, A. A. Nugroho, T. T. M. Palstra, M. W. Haverkort, **K. Wohlfeld**, M. Grüninger, **2013**, "Orbital superexchange and crystal field simultaneously at play in YVO_3: resonant inelastic x-ray scattering at the V L edge and the O K edge", **Physical Review B**, 88, 205115.

[e2] H. Y. Huang, C. J. Jia, Z. Y. Chen, **K. Wohlfeld**, B. Moritz, T. P. Devereaux, W. B. Wu, J. Okamoto, W. S. Lee, M. Hashimoto, Y. He, Z. X. Shen, Y. Yoshida, H. Eisaki, C. Y. Mou, C. T. Chen, and D. J. Huang, **2016**, "Raman and fluorescence characteristics of resonant inelastic X-ray scattering from doped superconducting cuprates", **Scientific Reports**, 6, 19657.

[e3] M. Rossi, M. Retegan, C. Giacobbe, R. Fumagalli, A. Efimenko, T. Kulka, **K. Wohlfeld**, A. I. Gubanov, and M. Moretti Sala, **2017**, "Possibility to realize spin-orbit-induced correlated physics in iridium fluorides", **Physical Review B**, 95, 235161.

In the papers mentioned above I was responsible for the reconciling of the experimentally observed physics either with the well-known previous theoretical results [e1, e3] or with the in-house theoretical data [e2]. Therefore I will just very briefly mention the main result of each paper:

- Paper [e1] shows that one of the orbital excitations found in the RIXS spectrum of the cubic vanadate (YVO_3) has a very weak dispersive feature which may probably be interpreted as an orbiton, though it cannot be reliably modelled using the appropriate superexchange model.
- Paper [e2] shows that the RIXS response on the cuprates is Raman-like in the spin channel and therefore, unless the opposite evidence exists, the spin excitations probed by RIXS could indeed be regarded as having a collective nature.

- Paper [e3] shows that, in contrast to previous theoretical proposals, the iridium fluorides are not 'ideal' examples of the Mott insulators with strong spin-orbit coupling: they should not be regarded as the 'pure' $j_{\text{eff}} = 1/2$ compounds and their low energy electronic excitations are not of collective nature.

(f) Persistence of Collective Spin Excitations in the Doped Hubbard Model [research after PhD]:

[f1] C. J. Jia, E. A. Nowadnick, **K. Wohlfeld**, C.-C. Chen, S. Johnston, T. Tohyama, B. Moritz, T. P. Devereaux, **2014**, "Persistent spin excitations in doped antiferromagnets revealed by resonant inelastic light scattering", **Nature Communications**, 5, 3314.

[f2] Y. F. Kung, C. Bazin, **K. Wohlfeld**, Yao Wang, C.-C. Chen, C. J. Jia, S. Johnston, B. Moritz, F. Mila, and T. P. Devereaux, **2017**, "Numerically exploring the 1D-2D dimensional crossover on spin dynamics in the doped Hubbard model", Physical Review B, 96, 195106.

One of the main results of the recent RIXS experiments concerns the collective spin excitations in the hole- and electron-doped copper oxides. In particular, the RIXS spectra on various copper oxides show almost no dependence on doping (even up to ca. 40% hole-doping) of the dispersion of the magnetic excitations along the $(0,0) \rightarrow (\pi,0)$ of the 2D Brillouin zone of the copper oxide planes. This is a striking results: Not only it had never been observed before these RIXS experiments, it is also completely counterintuitive – one expects that the nature of the collective magnetic excitations should by drastically different in the undoped and low-doped cuprates with magnetic long range order and in the optimally or overdoped cuprates with merely short range magnetic correlations.

Paper [f1] shows that the theoretically calculated RIXS cross section reproduces these peculiar RIXS experiments. Moreover, even just the spin dynamical structure factor of the Hubbard model, calculated using the quantum Monte Carlo methods, has the same feature. This counterintuitive result can partially be explained by invoking the so-called three-site terms: the correlated hopping that is present solely for the doped antiferromagnets and which leads to the persistence of the energy of the magnetic excitations upon doping. As discussed in [f2], such physics is not observed in 1D, where the three-site terms are relatively unimportant (due to the much lower number of possible three-site term paths in 1D than in 2D), but at the same time the nature of the collective magnetic excitations is completely different. However, gradually switching on the hopping between the 1D chains leads to the recovery of the 2D physics [f2].

(g) Theory of the Photoemission Spectra of Cuprates and Iridates [research after PhD]:

[g1] Y. Wang*, **K. Wohlfeld***, B. Moritz, C. J. Jia, M. van Veenendaal, K. Wu, C.-C. Chen, T. P. Devereaux, **2015**, "Origin of Strong Dispersion in Hubbard Insulators", **Physical Review B**, 92, 075119. [*Authors contributed equally]

[g2] E. M. Paerschke, **K. Wohlfeld**, K. Foyevtsova, J. van den Brink, **2017**, "Correlation induced electron-hole asymmetry in quasi-2D iridates", **Nature Communications**, 8, 686.

The crucial role played by the three-site terms in the understanding of the persistence of the collective spin excitations in doped cuprates [see point (f) above] has lead us to ask the following question: could the three-site terms matter not only for the spin but also for the electronic properties of the cuprates? To this end, in paper [g1] we calculated the single particle spectral function of the half-filled Hubbard model and compared it with the one calculated using the t–J model – with and without the usually neglected three-site terms. Using both exact diagonalization and self-consistent Born approximation, we unambiguously showed that a strongly dispersive feature, observable on the high-binding energy side of the photoemission spectrum of the Hubbard model, arises due to the three-site terms. As the low binding energy feature of the photoemission spectrum is due to the spin polaron physics, the high energy anomaly (the 'waterfall' feature), that is well known from the ARPES studies of the cuprates, finds a natural explanation within this model.

The study presented in [g1] has showed that the t–J model studies can be even more successful in reproducing the cuprate ARPES spectra than one had been expecting. Stimulated by this positive result, we studied in [g2] the photoemission and inverse photoemission spectra of the quasi-2D iridates (Sr_2IrO_4, Ba_2IrO_4). It turned out that the inverse photoemission spectrum of theses iridates qualitatively resembles the case of the quasi-2D cuprates: it can be modelled by a usual t–J like model. On the other hand, the photoemission spectrum requires a more complex model, which contains at least four different multiplet states per iridium ion site. This result has important consequences for the studies of the doped iridates: while the electron-doped iridates are qualitatively similar to the hole-doped cuprates, the hole-doped iridates are not like the electron-doped curpates and have to be modelled by a multiband Hubbard- or t–J–like model.

(h) Stability of Phases with Magnetic Long Range Order in Frustrated Systems [research after PhD]:

[h1] **K. Wohlfeld**, M. Daghofer, A. M. Oleś, **2011**, "Spin-orbital physics for p orbitals in alkali RO_2 hyperoxides — generalization of the Goodenough-Kanamori rules", **EPL (Europhysics Letters)**, 96, 27001.

[h2] D. Gotfryd, J. Rusnacko, **K. Wohlfeld**, G. Jackeli, J.Chaloupka, Andrzej M. Oleś, **2017**, "Phase diagram and spin correlations of the Kitaev-Heisenberg model: Importance of quantum effects", **Physical Review B**, 95, 024426.

Except for the studies presented in points (a-b) above, which solely concern the onset of the ordered ground states, most of the research presented in this review concerns the excited states of the correlated electron systems. Papers [h1-h2] present a somewhat different approach: by looking *inter alia* at the collective excited states of a particular correlated system in question, we investigate the stability of the long range ordered phase in the ground state.

In paper [h1] we try to understand how a long-range ordered magnetic state can be stabilized in a system that is frustrated – due to the geometry of the lattice as well as the orbital degeneracy of the ground state. We turn our attention to the alkali hyperoxides (RO_2, where R=Rb, K, or Cs) which are rather unusual systems with correlations and magnetic effects on the oxygen molecules that form a frustrated *bct* lattice. We derive an effective spin-orbital model for this compound and, using the linear spin wave theory, show that in general it does not support the long range order. The latter is due to the occurrence of the zero energy collective excitations for typical parameters of this system. The experimentally observed magnetic order can only be explained by invoking the Jahn-Teller effect.

In systems with strong on-site spin-orbit coupling, the orbital degrees of freedom usually do not enter explicitly, since the low energy models are more conveniently expressed in terms of the total angular momentum $j = l + s$ [see Sec. VIII of 4(c)]. Nevertheless, the interactions between the total angular momenta can still 'remember' about their orbital component and become very 'directional' or lead to frustrated models. Perhaps the best known example of such physics is found in the Kitaev-Heisenberg model on the honeycomb lattice, a model that describes the low energy physics of the '2-1-3' quasi-2D iridates (Na_2IrO_3, Li_2IrO_3). This model is inherently frustrated, which is best visible close to the so-called Kitaev points (i.e. when the Heisenberg interaction vanishes) with a spin liquid ground state. Paper [h2] investigates in detail the zero-temperature phase diagram of the Kitaev-Heisenberg model using the exact diagonalization combined with the cluster mean-field theory as well as the linear spin wave theory. We show and explain why out of the two different spin liquid phases that are stable in this model, the one with the ferromagnetic Kitaev interactions has a substantially broader range of stability than the one with the antiferromagnetic Kitaev interactions.